Rates and processes of stream bank erosion and its contribution to suspended sediment load, Big Spring Run, PA

Andrea Shilling
Earth and Environment Department
Franklin & Marshall College

Advisor: Dorothy Merritts, Earth and Environment
Franklin & Marshall College
GEO490: Independent Study
Project Submission: May 7, 2009
Graduation: May 15, 2010

Honors Thesis Defense Committee:
Dr. Allen Gellis, Research Hydrologist-Geomorphologist, USGS
Dr. Roger Thomas, Earth and Environment Department, Franklin & Marshall College
Dr. Andy DeWet, Earth and Environment Department, Franklin & Marshall College

Contents

ABSTRACT 2
INTRODUCTION 3
BACKGROUND 4
Climate, Topography, and Geologic Setting 4
Site History 5
Sediment Budgets 7
Stream Bank Erosion 8
Needle Ice 9
METHODS 11
Digital Orthophotographs 12
Erosion Pins 13
Cross Sections 14
Geomorphic Mapping of Stream Banks 14
Lidar 16
Calculating Erosion Rates, Volume, and Mass 16
Identifying Freeze-Thaw Cycles 17
Bulk Density Determination 18
Procedure for Grain Size Analysis 18
RESULTS 19
Mapping Stream Banks and Processes of Erosion and Deposition 19
Determining Volume and Mass of Eroded and Deposited Stream Bank Sediment 22
DISCUSSION 25
CONCLUSIONS 31
ACKNOWLEDGEMENTS 33
REFERENCES 34
FIGURES LIST 36

ABSTRACT

Part of the headwaters of Big Spring Run (BSR), a tributary to Mill creek in Lancaster County, was studied to determine key components of a sediment budget. This area has a history of dam use that is documented in historic maps, photographs, and public records, and is evident by the presence of historic sediment that accumulated along the valley bottom. These early dams have been breached, and the modern BSR channel has incised through this sediment. Several methods were used to measure the rates of change (erosion and deposition) in position of the modern channel and to aid in the development of a sediment budget. These methods include stream bank mapping in the field and on repeat digital orthophotos, repeat measurements of bank pins, and repeat surveys of cross sections. Three types of stream banks were mapped along 1.4 km of BSR. Type 1a and 1b banks had the highest rates of erosion and differed slightly from one another by bank height and composition. Type 1a banks have an average height of 1.1 m and consist of >80% silt and clay, while Type 1b banks have an average height of 0.9 m, a higher sand content, and some gravel. Type 2 banks showed little to no erosion or deposition during the study period. Type 3 banks demonstrate active deposition.

From repeated measurements of bank pins over one to two years, the rate of erosion was 23.9 cm/yr for Type 1a banks and 31.1 cm/yr for Type 1b banks. It was difficult to measure the rate of deposition on Type 3 banks with pins because many of the pins were buried during the measurement period. Cross sections were used to calculate rates of change in the bank position over a period of six years. Twelve cross sections were surveyed in 2004 and again in April of 2010. For bank Types 1a and 1b, rates of bank erosion determined from the cross sections (0 to 21.2 cm/yr) overlap the lower values measured with pins. Both the pins and cross sections show that Type 1a and 1b banks are actively eroding at a higher rate than other bank types. The data show that Type 2 banks were eroding and depositing at different sites during the 6 years; however, the rates of change for this bank type were lower than for all other types. Overall, there was little change in Type 2 banks over the six-year monitoring period. Type 3 banks showed active deposition in both the pin and cross section data.

This study supports the hypothesis that stream banks can be a major source of sediment for a stream that is incised into fine-grained (silt and clay) sediment. Provisional USGS gage station data provided by Dr. Michael Langland show that the majority of suspended sediment transport occurs during the months of April through August. The bank material at BSR, mostly silt and clay, makes the banks especially prone to erosion by subaerial processes, particularly freeze-thaw and needle ice formation. Both processes were observed during the study period. The actual entrainment of sediment and its subsequent downstream transport appear to be associated with high flow events. Whereas sediment is shed from banks at a relatively high rate during the winter months of December through March by freeze-thaw processes, the peak period of sediment transport measured at the USGS gage at the downstream end of the study reach occurs up to five months later. The results of the stream bank study presented here indicate that as much as 111 to 144 tons/yr of sediment is deposited in the study reach between two gage stations located at the upstream ends of two tributaries entering the study reach and one gage station at the downstream end of the main stem in the study reach. If so, then an amount equivalent to most, or possibly all, of the incoming 138 tons of sediment measured at the two upstream gages might be deposited in the study reach. Accounting for this deposition, some 130

to 151 tons/yr of sediment must be eroded from the study reach in order to supply the 157 tons/yr measured at the downstream gage.

INTRODUCTION

This paper presents the results of research focused on quantifying key elements of a sediment budget for a portion of the Big Spring Run (BSR) watershed (Figure 1). The objective of this research is to measure the amount of fine-grained sediment eroded and deposited along stream banks within the study reach, and to compare this amount to the flux of fine-grained sediment measured at U. S. Geological Survey (USGS) gage stations located up and down stream of this reach.

The field site spans a 1.4-km long reach of the BSR watershed near the town of Willow Valley in Lancaster County, Pennsylvania. The study reach includes two headwater tributaries and a portion of the main stem of BSR downstream of their confluence. Beyond the study reach, BSR continues 1.5 km northward before joining Mill Creek, a tributary to the Conestoga River. The Conestoga River, in turn, empties into the Susquehanna River, one of the largest tributaries to the Chesapeake Bay. The Conestoga has been identified as one of the tributaries with high suspended sediment loads within the Chesapeake Bay watershed (Gellis et al, 2004).

BSR is included on the United States Environmental Protection Agency's Clean Water Act section 303 (d) list of impaired water bodies because of high loads of suspended sediments and nutrients (Voli et al, 2009). The study reach is the site of ongoing research by scientists, groups from Franklin & Marshall College, Pennsylvania Department of Environmental Protection, the United States Geologic Survey, and the United States Environmental Protection Agency. This team of collaborators is working to assess a floodplain, stream, and riparian wetland restoration approach to ecological restoration.

Three gage stations established by the USGS in September, 2008, collect data at 5-minute intervals on gage height, water temperature, and turbidity from fine-grained (suspended) sediment, and record data at 15-minute intervals (see Figure 1 for locations of the three gage stations). One gage station is located at the upstream end of each of the two headwater tributaries just above the study reach. The third station is located at the downstream end of the main stem just below the study reach. During high-flow events, an ISCO sampler collects suspended sediment at 15- to 30-minute intervals. Data from these stations are compared with bank erosion measured in this study in order to evaluate the contribution of stream bank erosion to the suspended sediment load in BSR.

BACKGROUND

Climate, Topography, and Geologic Setting

The climate of the BSR study site is humid-temperate, with an average annual precipitation of 104 cm (41 inches) and average annual temperature of 11°C (52°F) (Galeone et al, 2006). Rainfall is distributed relatively evenly throughout the year, with some rain from occasional hurricanes during summer and fall months. The year 2009 was unusually wet, with total rainfall of 167.1 cm (65.8 inches) and total snowfall of 92.7 cm (36.5 inches). Daily high temperatures were below freezing for a total of 24 days in 2009, and daily low temperatures were below freezing for 100 days in 2009 (Table 1). As of March 2010, an additional 16 days had high temperatures below freezing and 65 days had low temperatures below freezing (Millersville University Weather Information Center, http://www.atmos.millersville.edu/~wic/).

The topography of the BSR region is one of low to moderate relief with broad rolling hills and valleys (Galeone et al, 2006; see Figure 2 for a topographic map of BSR). The

maximum elevation in the BSR watershed is 151.7 m and the minimum elevation, at the mouth of the stream where it joins Mill Creek, is 81 m. The relief for the watershed is about 60 m (Figure 3).

Beginning at multiple springs, BSR flows northward over weathered Paleozoic limestone (Galeone et al, 2006). This limestone is mapped on the Quarryville and Conestoga geologic quadrangles as the Cambrian to Ordovician age Conestoga Formation (Blackmer, 2007). The Conestoga Formation consists of light to medium gray crystalline limestone with phyllitic partings and medium gray phyllitic limestone (Blackmer, 2007). Numerous quartz veins that vary in thickness from several mm to as much as a meter are common in the Conestoga Formation. Variable amounts of mica (muscovite and phlogopite) and common accessory minerals such as pyrite also occur in the Conestoga Formation (Blackmer, 2007). The USGS reports that the study site lies within the southern part of the Lancaster belt, an area of structural complexity that has undergone repeated deformation, faulting, and isoclinal folding (Galeone et al, 2006). The PA Geologic Survey (Blackmer, 2007) reports that median groundwater yield for the Conestoga Formation is 25 gal/min, although solution openings may produce higher yields.

Site History

A study of seed types preserved in the sediments and age dating of paleosols along BSR determined its Holocene paleogeography (Voli et al, 2009). The results of this study showed that the valley supported an herbaceous wet meadow that persisted from approximately 3,200 to ~300 yrs BP. It is likely that multiple springs along the valley bottom and margins maintained the saturated condition of this ecologically resilient wetland.

After the arrival of European settlers circa 1730 AD, land clearing and milldam construction initiated a period of sedimentation along the valley bottom (Walter and Merritts,

2008). This historic sedimentation buried the Holocene wetland (Voli et al, 2009). Alexandra Sullivan (F&M '06) investigated the history of land use in the BSR watershed. One 3-m high milldam near the mouth of BSR was built in the 1700s and operated a mill until the early 20th century. Many small dams also were built along BSR for purposes such as ice harvesting and as farm ponds. Remnants of these dams are found along eroding stream banks, and local farmers have photographs of ponds from the early 20th century. In addition, bridges and road crossing created constrictions that impacted stream flow and sediment transport. As the valley bottom filled with sediment, some farmers shifted segments of the stream toward the valley margins to create more pasture or farm land. Mr. Harlan Keener, the owner of the farm that begins at the northern boundary of the study reach, described how his grandfather straightened the main stem of BSR and relocated it to the west, along the valley margin, with a team of horses in 1916. The flat land adjacent to the stream is referred to as "bottom land" by local farmers. Mr. Keener also reported that he once found a log structure that might have been associated with early wetland drainage. In addition, as the stream incised into historic sediment some farmers used boulders and other coarse material to control erosion that occurred along stream banks. Finally, a sewer line was laid along BSR in the mid-20th century. Its construction involved bedrock excavation and relocation of part of the channel within the study reach.

Merritts (unpub. data, 2010) used historic maps and photographs to determine that stream incision began in the study reach before 1940 and perhaps as early as 1890. This suggests that early dams were breached or removed prior to the early 20th century. As a result, the pre-settlement wetland soil is exposed along the bases of incised stream banks as a dark layer of sediment distinct from the lighter colored historic sediment that overlies it. In general, the post-settlement sediment is thickest near the valley center and pinches out laterally along valley

margins. It generally thickens downstream toward road crossings, milldams, and other constrictions that produced slackwater effects and sedimentation (unpub. field mapping and data, Merritts, 2010).

Sediment Budgets

A sediment budget is a quantitative means of evaluating rates of sediment production, transport, storage, and discharge in a watershed (c.f., Dietrich et al, 1982). A full budget for a drainage basin measures the amount of sediment produced in a system by erosion, the amount transported and stored throughout the watershed, and the amount that exits the watershed. A sediment budget for a watershed typically includes the following components:

- Hillslope erosion (e.g, by sheetwash and mass movement)
- Colluvial hollow infilling
- Alluvial fan deposition
- Streambank erosion
- Channel bed scour
- Floodplain and bar deposition
- Suspended and bed load sediment discharge in a stream channel

In a simple example, sediment might be eroded from a hill slope, stored temporarily on a bar, and then transported out of the system as bed load. In a sediment budget analysis, the actual amounts and rates of each of these components would be measured.

Sediment budgets can be determined for a whole watershed or a particular stream reach (c.f., Allmendinger et al, 2007). They are useful for evaluating the contribution of different

sediment sources, such as upland slopes versus stream banks, to the total load of sediment in a stream.

Stream Bank Erosion

Wynn et al (2007) describe stream bank erosion—the net removal of sediment from the bank--as the result of multiple processes working in conjunction to cause stream bank retreat (Table 2 for a list of important terms and definitions). The three primary mechanisms of bank erosion include mass wasting, fluvial entrainment, and subaerial processes (Lawler et al, 1997; Simon et al, 2000; Wynn et al, 2008) (Table 3 lists examples of the different erosion processes).

Mass movement processes include bank collapse, calving, slumping, and toppling. Fluvial processes remove sediment when water flowing past the bank entrains sediment. Subaerial processes include such events as wetting and drying or freezing and thawing, both of which lead to lower bank shear strength. These processes often are considered secondary because they lead to an increase in soil erodibility. They also are referred to as preparatory processes (Lawler, 1986; Wynn et al, 2008). This last category has received more attention recently and many studies have shown that stream bank erosion increases significantly following the action of subaerial processes (Lawler, 1986; Wynn et al, 2008).

Several studies have determined that the majority of bank erosion occurs in the winter months, from November/December to March/April, whereas little erosion occurs during summer months (Wolman, 1959; Lawler, 1988; and Wynn et al, 2008). Wolman (1959) found that high flows combined with thoroughly wetted banks resulted in the highest rates of erosion. Wynn et al (2008) reported that higher erodibility of banks in winter compared to spring/fall and summer is due in large part (80%) to freeze-thaw cycling that disaggregates bank material.

Some forms of stream bank erosion cannot be observed directly, but rather are noted through observations of certain features. Examples include tension cracking at the top of the bank and failed blocks of bank material at the bottom of the bank. Lawler et al (1997) found that the presence of an overhang suggests that flows below bankful level are able to cause erosion by fluvial entrainment. Subaerial processes such as freeze-thaw in the winter or desiccation in the summer can cause an accumulation of sediment at the base of the bank. High water notches in these "aprons" of debris show that fluvial entrainment has removed sediment.

Cohesive banks composed primarily of silt and clay are typically more susceptible to subaerial erosion then less cohesive banks composed of coarser grained sediment (Lawler et al, 1997). While numerous processes can increase the erodibility of cohesive banks, the three main processes identified by Lawler et al (1997) are pre-wetting, desiccation, and freeze-thaw activity. Two figures from Couper (2003) illustrate this point. The first, Figure 4, illustrates the process of subaerial transfer of sediment to the lower bank where the sediment is removed by fluvial entrainment. A second figure from Couper (2003) shows that bank erodibility increases with silt-clay content (Figure 5). It is important to note that cohesive banks tend not to erode as individual particles, but rather as aggregated clumps and large masses (Lawler et al, 1997).

Needle Ice

A common subaerial process that disaggregates bank material is associated with the formation of needle ice (Figure 6). Needle ice is a cryergenic phenomenon that occurs when conditions are right for the formation of needles of ice within soil. Needle ice has been described by Washburn (1979:92) as the "accumulation of slender, bristle-like ice crystals", or needles, either at or just below the ground surface. These filaments of ice are about 1 mm^2 in cross

section diameter, and up to 10 cm in length (Outcalt, 1971; and Lawler, 1988). Needle ice is considered to form during the winter. It forms after daylight hours, when the ground is unfrozen or thawed, and during evening hours with clear skies. At such times, the ground surface is likely to be cooler than under other conditions (Outcalt, 1971; and Lawler, 1988).

The amount of moisture and the temperature are the two main controlling factors in needle ice formation (Lawler, 1988). The duration of freezing, or amount of time over which the needle ice forms, controls needle length and this in turn is related to sediment concentration (ppm, or mg/L) (Lawler, 1988). Wolman (1959) reports that frost action (needle ice) acts not only to hold moisture in the banks, but also to break apart the surface material into increasingly smaller pieces, making it easier to erode during the high flows with spring rain. Lawler (1993) reports that a combined sequence of needle ice growth and high flow appears to be a significant means of bank erosion.

Needle ice not only prepares banks for erosion, but also acts as a direct mechanism of erosion (Wolman, 1959; Lawler, 1988). Needle ice does not always form over the course of one night. If growth takes place over many nights, multiple layers build up, adding to the thickness of 'polycyclic' needle ice (Lawler, 1993). In order for this type of needle ice to occur, partial rather than complete melting, of the needle ice must take place (Lawler, 1993). When needles of ice form over multiple days small amounts of sediment become trapped within the needles, often as visible bands. When partial melting occurs during the day, sediment becomes incorporated into the needles when refreezing takes place at night (Lawler, 1993). Sediment captured in this way appears as bands in the needles. This sediment is transferred into the stream when needle ice melts and sediment flows down the bank and into the water (Figure 7; Lawler, 1993).

In a study of the River Ilston, in the UK, Lawler (1993) estimated that 32-43% of total bank retreat was a result of needle ice formation (Wynn et al., 2008). Lawler (1993) reports that needle ice serves both an indirect and distributing role in weakening the bank structure and increasing the store of erodible sediment.

METHODS

Several methods were used to obtain the information needed to evaluate the contribution of stream bank erosion to total suspended sediment load for the study reach at BSR. The information needed to evaluate stream bank erosion includes the following:

- total suspended sediment load entering the study reach
- total suspended sediment load exiting the reach
- rate of bank erosion
- rate of deposition (storage) within the study reach

The first two fluxes were measured by the USGS, and the second two were the focus of this study. As noted above, in August and September of 2008, the USGS established two stream gage stations to determine the suspended sediment load at the upstream ends of the two tributaries which mark the beginning of the study reach (see Figure 1 for the locations of the gage stations). At the same time, a third gage station was established on the main stem at the downstream end of the study reach. At all three of these stations, the USGS has collected continuous data on turbidity from October, 2008, to present, and during storm flow sampled stream water in order to determine the flux of fine sediment into and out of the study reach.

In this study, four approaches were used to determine rates of bank erosion and deposition. These included analysis of repeat digital orthophotographs, measurement of bank pins, resurveying of channel cross sections, and mapping of stream banks based on geomorphic characteristics. In addition, the processes of bank erosion were investigated by frequent visits to the field site under different conditions (e.g., storm flow, low flow, cold, snow, etc), repeat photography at monumented stations, and analysis of moisture content and temperature of the stream bank determined by sensors installed at one site. High-resolution topographic data for the entire BSR watershed was obtained with airborne laser swath mapping, also known as lidar (light detection and ranging) in October, 2008, from the National Center for Airborne Laser Mapping (NCALM). This high-resolution topographic data was useful for evaluating the positions of bank edges.

Digital Orthophotographs

Digital orthoimages from 2001, 2005, and 2008 were obtained and evaluated in a GIS database in ArcMap. The horizontal resolutions of these images are 2 ft (2001) and 1 ft (2005 and 2008). Accuracy for the 2005 and 2008 images is quantified as having maximum root mean square deviation (RMSE) of 95% for check points within 5.0 ft or better. Accuracy for the 2001 images was not quantified, but probably is about ±1.5 m.

In the GIS environment, the banks of the stream were traced for each year and assigned a color. Outlining the stream banks for each year and then comparing these mapped stream segments allowed changes in stream banks to be observed. While it is possible to see general trends through this method, smaller changes are not detectible. The resolution of the photographs, particularly the 2001 orthophotograph, is not sufficient to allow small changes (<1 m) that occurred over the three and four-year intervals to be measured.

Erosion Pins

Erosion pins were installed at different stream bank locations of BSR over the course of two years. Data has been collected on each pin since installation (Figures 8 and 9). When the pins were first installed the distance from the top of the bank to each pin was measured and recorded. The erosion pins, which consist of ¼-inch diameter rebar stakes measuring 4 ft in length, are pounded into the bank leaving a certain length exposed. Some of the early pins used were 2 ft in length. These were replaced with 4-ft pins within a year. When originally installed the amount of pin left exposed was recorded and every time the pin was measured the data were compiled in an excel spreadsheet. From May 2008 to September 2009, pins were installed and monitored at 35 sites along BSR. At each of these sites three (sometimes four) pins were installed in an evenly spaced line from the top of the bank to water level. Pins were measured at intervals of about one time per month with a cm-scale ruler. Measurement error is estimated to be ~±1 cm.

At two locations (referred to as the "Type Locality" and the "Houser Grid" sites) a grid of pins was installed to more closely monitor bank erosion. The Type Locality site has seven columns of pins with three pins in each column (see Figure 1 for the location of the "Type Locality"). The columns and pins were installed at equally spaced, regular intervals (~1 m apart). Five of these rows were installed at the start of this research project and two were installed in 2008. At the Houser Grid site, located ~300 m upstream of the study reach on the eastern tributary of BSR, five equally spaced columns of pins were installed across the bank face (~1 m apart) and the pins within each column were equally spaced vertically on the face (Figure 10).

Once the data were compiled, and cumulative amounts calculated the rate of erosion was calculated in both cm/day and cm/yr. This was done first by calculating the amount of erosion measured each time and then adding those values together for a cumulative amount of erosion. This value was divided by the total number of days the pin had been in the bank, yielding the rate of erosion per day. Multiplying this value by 365 gave the rate of erosion in cm/year. A buried pin was recorded as having 0 cm of pin exposed if we could see the tip of the pin; otherwise the amount of erosion was left blank. If a pin was lost then a new pin was installed at the same distance from the top of the bank and the new distance exposed was recorded. Calculations started over with the reinstallation of any pins since there is no way to determine when the pin fell out or how much additional erosion of the bank might have occurred after the loss of the pin. If any pin was buried for too long, then data was no longer recorded for that pin. It is for this reason that so few pins were available to measure for areas of deposition.

Cross Sections

A series of 12 cross sections at BSR was surveyed with a total geodetic station by LandStudies, Inc., surveyors in 2004 (Figure 11). The cross sections were surveyed again with a Trimble RTK-GPS unit by Michael Rahnis in April 2010. By comparing the 2004 cross sections to the cross sections collected in 2010, it is possible to measure the area of bank erosion and deposition, and from these areas to calculate rates of change. See Appendix 1 for a more detailed description of the cross section surveying methods.

Geomorphic Mapping of Stream Banks

From January to March, 2010, bank types were mapped throughout the study area based on their geomorphic expression and evidence of erosion or deposition. Bank height from

channel bed to top of bank was measured with a stadia rod for each mapped bank segment. While mapping the banks, banks were photographed and observations of the different types of erosion were recorded.

Three bank types were identified and labeled as Types 1a, 1b, 2, and 3 (Figure 12). Type 1a banks contain >80-90% silt and clay and have vertical to near vertical bank faces that appear to be highly erodible. Sub-vertical fractures parallel to the bank face are common in this bank type. This bank type is common along the outside of meander bends. Type 1b is the same as Type 1a but has a higher content of sand and, locally, some gravel. In addition, Type 1b banks are slightly lower than Type 1a banks and younger in depositional age. They were deposited within the stream corridor since incision into the fine sediment that comprises bank Type 1a. Minor amounts of plastic and aluminum trash have been found in Type 1b banks. Type 2 banks are hummocky, typically vegetated with grasses, and most common along straight reaches of the BSR channel. In many places, the hummocky masses are slump blocks that are not yet completely disintegrated. Type 2 banks have irregular bank heights and evidence of both erosion and deposition, although neither is as notable as for Type 1a, 1b, and 3 banks. Type 3 banks are common along the inside of meander bends. Type 3 banks have higher sand and gravel content and more gently sloping banks (low bank angle) than all other bank types, with clear evidence of recent, ongoing deposition during moderate to high flow events.

Stream bank segments mapped in the field were transferred to a GIS (ArcMap) database using the 2008 digital orthophotos as a map base. Each bank type was assigned a color to allow for trends to be observed easily and bank lengths to be calculated. The resulting line segments in ArcMap were measured in order to determine the total length of each type of stream bank. The field data for bank height was added as an attribute for each mapped segment. For some bank

segments the bank height was difficult to measure in the field and was measured instead from the lidar data, as discussed below.

Lidar

The lidar data used for this research were acquired by NCALM in 2008. When it proved difficult to get accurate bank heights in the field either due to vegetation overgrowth or hummocky banks, lidar data were analyzed in GIS. Several topographic profiles were drawn across the stream channel, the heights of the bank determined, and an average bank height calculated. The lidar also was useful in acquiring general topographic data, including elevation variations, maximum height, minimum height, and slope.

Calculating Erosion Rates, Volume, and Mass

The rate and amount of sediment eroded from bank Types 1a and 1b were calculated in three different ways. For the first method, the length of stream bank was multiplied by the average height for each bank type in order to get the area of bank eroded. To calculate volume of sediment eroded, each bank area was multiplied by the average annual rate of erosion determined for that bank type from the pin data. The volume then was multiplied by bulk density in order to get mass of sediment eroded. Minimum and maximum values of bulk density measured for Big Spring Run samples by previous Franklin and Marshall College student researchers were used. These values are 1000 and 1300 kg/m^3, respectively, determined by Zach Stein (2008), Stacey Sosenko (2009), and Chris Fullinwider (2010).

The second method of calculation was similar to the first, but the area of each individual bank segment was calculated. Bank heights measured for each segment in the field and the length of each segment as measured on the 2008 digital orthophotos were multiplied. The individual segment areas were added together for a total area of erosion for Types 1a and 1b. As

with the first approach, the bank area was multiplied by the average annual erosion rate determined from the bank pin data in order to obtain volume of eroded sediment. This volume was converted to mass, as before, by multiplying it with the range of minimum to maximum measured bulk densities.

Surveyed cross section data were used in the third method of calculating volume and mass of eroded sediment. The area of erosion for each cross-section that included a Type 1a bank was calculated by measuring the average area of erosion that had occurred from 2004 to 2010, the time span represented by the beginning and ending surveys (Figure 13). An average of the area of erosion for all cross sections was determined and multiplied by the length of Type 1a banks, yielding total volume eroded in cubic meters. This estimate of eroded volume was converted to tons, as for the previous two methods, using a range of bulk density values. This estimate of erosion was divided by six to obtain an average annual rate of erosion.

Volume of deposition within the study reach was also calculated using the third method. Bank pins are not useful for measuring active deposition, as they are buried frequently and difficult to find. The cross sections provided the only means to calculate deposition. As in calculating rates of erosion, the average height and width of each deposit were measured to calculate area. An average area was determined from all cross sections with a Type 3 bank and multiplied by the total length of this bank type, yielding volume of deposited sediment. As done for estimates of eroded sediment, this value was converted to tons by multiplying it with the range of measured bulk densities.

Identifying Freeze-Thaw Cycles

The presence of freeze-thaw cycles was detected both through field observations and with the use of HOBO sensors with a data logger. During repeated field visits bank sediment was

examined for the presence of needle ice. The HOBO datalogger was attached to two soil temperature probes and two moisture content probes (Figure 14). One temperature sensor and a moisture content sensor were installed approximately 0.5 m above water level along the exposed east-facing stream bank at the "type locality", and a second set of sensors was installed ~0.3 m above the first pair. The HOBO sensors and data logger were set to record information every three minutes. The instruments were installed in November, 2009, and the data downloaded and analyzed in early April, 2010.

Bulk Density Determination

Bulk density was measured for samples of bank material for Type 1a, 1b, and 3 banks. The procedure used was to weigh 900 mL of sediment (field moist and air dried condition) lightly packed in a 1000 mL beaker. To calculate bulk density, this weight is divided by the volume, 900 mL.

Procedure for Grain Size Analysis

To determine the percent mass of clay, silt, sand, and gravel in sediment samples from BSR, roughly 500 g of sample is placed on clean, unused paper sheets and left at room temperature until dry (ca. one week). Once dried, the sample is thoroughly mixed and split into four equivalent aliquots. One aliquot is weighed, and its mass recorded. This sample is lightly pulverized using a ceramic mortar and pestle, then sieved using 38.1 mm, 19.0 mm, 9.51 mm, 4.699 mm, 2.00 mm, 0.59436 mm, 0.2972 mm, 0.14986 mm, and 0.0635 mm mesh screens. Material greater than 2 mm is cobbles, pebbles, and granules, in order of decreasing sieve size. Particles of cobbles, pebbles, and granules are weighed separately and their masses recorded. The < 2 mm fractions are inspected under a binocular microscope, re-pulverized, and sieved, if necessary, in order to disaggregate clumped grains. The < 2-mm size fractions are weighed

separately and individual masses recorded. The masses for all size fractions are summed, and this value is used as the total mass of the sample.

The percent clay, silt, and very fine to medium sand are determined with a Micromeritics Saturn DigiSizer 5200 Laser Particle Analyzer (LPA). A small (ca. 1 g) sample of the -50 mesh fraction (i.e., sample below 0.2972 mm) is placed in the sample chamber of a Micromeritics Saturn laser particle analyzer (LPA). The LPA provides an estimate of particle size distributions from ~ 300 microns to ca 1 micron. After LPA analysis, the data are merged with the sieve data in a pre-formatted excel spreadsheet (Laura Kratz, personal communication). Once the data are merged, a report of the grain size distribution is generated for the bulk sample, yielding percent cobble, pebble, granule, sand (coarse to very fine), silt, and clay.

RESULTS

Mapping Stream Banks and Processes of Erosion and Deposition

Figure 15 shows the 2008 orthoimage with the four mapped bank types. Each color corresponds to one of the types (see Figure 12 for images of each bank type). Table 4 summarizes the length of each bank type. The majority of banks can be characterized as Type 2 (994 m in length). Together types 1a and 1b comprise 952 m of the stream bank length (Figure 16). Type 3 comprises 671 m of bank length (Figure 17). Approximately 74 m of the stream banks were mapped as rubble. Most of this rubble is boulders that protect a buried sewer line; these boulders have been exposed by bank erosion.

The highest banks were Type 1a, with an average height of 1.2 m. This average height generally diminishes upstream of the confluence of the main stem with its two tributaries, because BSR is incised into historic fill that thins upstream. This fill, as well as the underlying

original valley bottom, is exposed along the faces of bank Type 1a. The average height of Type 1b banks, 1.1 m, is slightly less than Type 1a, and most Type 1b banks occur downstream of the tributary confluence. Bank Type 2 had an average height of 1.0 m. (See Appendix 2 for additional bank height information). The height of Type 3 banks, which are depositional landforms, could not be measured in the field because their height diminishes toward the channel, approaching zero at water level. The height of these depositional features is not required for the estimates of erosion presented below.

The mapping of banks was done in the winter, so no observations regarding the types of erosion that might occur during the summer were made; however photos of BSR taken at different times during the past five years by D. Merritts, R. Walter, and C. Shenk show evidence of desiccation and fracturing of the banks during the summer.

Erosional processes were observed during frequent visits to the field site from September 2009 to April 2010. These visits were timed to correspond with pre- and post-storm periods as well as periods of possible freeze-thaw in order to look for evidence of erosion. Numerous examples of subaerial processes were observed. Figures 18 & 19 show evidence of recent mass movement and Figure 20 shows a slump block at the "Type Locality" that occurred sometime between 12/6/2010 and 12/17/2010. Large slump blocks were observed on numerous occasions. These blocks were observed shortly (generally within 2 to 3 days) after the water stage dropped at the end of a high-flow event. This change in stage, from high to low, leads to mass movement because banks are wetted during high stage and the falling stage results in a rapid change in pore pressure (c.f., Simon et al, 2000).

While in the field during the winter of 2009-2010, numerous examples of needle ice acting as both primary and secondary sources of erosion were observed and photographed. The

primary mechanisms of needle ice erosion were discussed earlier (see Figure 9). At several sites and during multiple visits, needle ice was observed pushing sediment outward from the bank. As seen in Figure 21, some of the sediment fell from the bank face directly into the water. In this way, needle ice acts as a primary source of erosion. Needle ice acts as a secondary means of erosion when it loosens sediments and prepares it for subsequent erosion.

While numerous examples of this process of secondary subaerial erosion were observed, the bank face shown in Figure 22 illustrates this process particularly well. Not only can the apron of sediment produced by the needle ice be seen, but also it is evident that some of the sediment was removed from the base of the apron in a recent high flow event. This removal of sediment by water flow is evidence of fluvial entrainment.

Aside from visual observations of needle ice, evidence of freeze-thaw events was detected with the two HOBO sensors that monitored the temperature and moisture content of the east-facing bank face at the "Type Locality". A similar method was used by Wynn et al (2008) to detect freeze thaw events from temperature and soil moisture content. According to Wynn et al (2008), a temperature decrease that is accompanied by a sudden decrease in moisture content is a sign of a freeze-thaw event. As moisture in the sediment freezes, it no longer is detected by the sensor, so the moisture content drops. Sensor data from a 5-day period from January 8 to 13, 2010, exhibits several freeze thaw events (Figure 23). Note that as temperature drops, so does the moisture content of the bank (compare to Figure 5 in Wynn et al, 2008).

The sensor data indicate that freeze-thaw events began in early December and continued at least until mid-March, the most recent date examined in this study. Local weather data indicate that air temperature fell below freezing at least 97 times during this same period.

Determining Volume and Mass of Eroded and Deposited Stream Bank Sediment

Examples of bank erosion observed by tracing bank edges on digital orthoimages from 2001, 2005, and 2008 are shown in Figure 24. Aerial photographs of BSR taken with a remotely controlled airplane in 2006 also were used to visually assess the amount of bank retreat over 4 years (Figure 25). These aerial photographs support observations of erosion along bank edges as mapped on digital orthophotos from 2001, 2005, and 2008. Figure 26 is an aerial photograph taken in 2006 of a meander bend of BSR that was eroded as shown in Image D of Figure 24. Table 5 summarizes the type of bank at each erosion pin site, the identification number for each site (corresponding to the maps in Figures 8 and 9), the average annual erosion rate for each site (three to four pins per site, at top, middle, and bottom of bank), and the average annual erosion rate for all pins representing each bank type.

For Method 1, the average height of all Type 1a banks (1.2 m) was calculated and multiplied by the total length of bank Type 1a (765 m), yielding a bank area of 918 m^2. This area then was multiplied by the average erosion rate (0.24 m/yr) for the pins in Type 1a banks. The resulting volume is 219.4 m^3. The same procedure was used for Type 1b banks. The average bank height of 1.1 m multiplied by the total bank length (187 m) resulted in an area of 205.7 m^2. This area then was multiplied by the average rate of erosion (0.31 m/yr) calculated for Type 1b, resulting in a volume of 64.4 m^3. The two volumes for Types 1a and 1b were added together and the resulting total, 283.8 m^3/yr, was multiplied by bulk density to determine mass in kg. A range of bulk density values, from 1000 kg/m^3 to 1300 kg/m^3, represents the range determined for bank samples from BSR. This range in mass values then was converted to tons. The resulting values of erosion for bank Types 1a and 1b were 312.8 to 406.7 tons/yr.

For Method 2, the area of each segment of bank mapped as Type 1a or 1b was calculated from individual segment heights and lengths. All of the areas for Type 1a were added together (992.3 m^2). This average then was multiplied by the average erosion rate for Type 1a (0.24 m/yr), resulting in a volume of 237.2 m^3/yr. The same was done for all the segments classified as Type 1b; the total area for this bank type is 201.2 m^2. This area then was multiplied by the average erosion rate (0.31 m/yr) for bank Type 1b, resulting in a volume of 63.0 m^3/year. These two volumes were summed to obtain a total volume of erosion, 300.1 m^3/yr, which was multiplied by the two different bulk densities, as in Method 1, to convert to tons. The final estimate of eroded mass of sediment is 330.8 to 430.1 tons/yr.

Method 3 was used to calculate rates of erosion and deposition based on stream channel changes detected in cross section surveys done in 2004 and 2010. Using the two surveys, it was possible to calculate the area of deposition or erosion (see Figure 13). No cross section transected a Type 1b bank, so the average area of 0.7 m^2 for Type 1a was multiplied by the total length of both Type 1a and 1b banks (952 m) to determine the volume per year, 158.7 m^3. This volume then was multiplied by the range in bulk densities, as in the previous two methods, yielding estimates of mass of eroded sediment that range from 175 to 227 tons/yr. The area and mass of deposition was calculated in the same manner as erosion resulting in an average area of 0.15 m^2 which was multiplied by the total length of 671 m. This volume, 100.7 m^3/yr, was multiplied by the two different bulk densities, as in the previous two methods, resulting in a range of 111.0 to 144.3 tons/yr of eroded sediment from Type 1a and 1b banks.

Figures representing six years of change are shown for all cross sections in Appendix 3. Table 6 summarizes the data collected for each cross section (see Figure 11 for location map of cross sections). Table 7 includes the information used to calculate an average volume of erosion

per year, which then was used to calculate erosion in tons per year. This table includes the bank type for each cross section, the amount of lateral bank retreat and advance, the amount of vertical change, and the rates of retreat, advance, and vertical change. In this discussion, bank retreat refers to erosion and is indicated with negative values, whereas bank advance refers to deposition and is indicated with positive values.

The average rate of change in bank position, the minimum and maximum rates of change, one standard deviation (σ), and $\pm\sigma$ for both the pin and cross section data are organized by bank type in Table 8. In Figure 27, pin and cross section data are compared for each bank type. The graphs are set to the same scale and stacked one above the other in order to show trends for the different bank types. The average rate for each data series is shown in red, and the two red lines in each series represent one standard deviation from the average.

Grain size analysis of sediment that comprises three of the four bank types (1a, 1b, and 3) indicates that the historic sediment in which the modern BSR channel is incised is mostly silt and clay (Figures 28 and 29). This material comprises the exposures of bank Type 1a. The younger inset alluvium in which Type 1b banks are formed is coarser, with more sand and sometimes gravel. Field observations and data from one sample site indicate that the sediment deposited at Type 3 banks on the inside of meander bends is notably coarser than sediment in both Type 1a and 1b banks. The source of the gravel that is deposited during storm flow events appears is a Pleistocene sandy gravel that underlies the historic sediment (unpub. data, Merritts and Walter). At scoured areas along the channel bed, as at the "Type Locality", sand, granules, and pebbles have been winnowed from the bed, leaving an armored cobble lag. In addition, the channel is located along the valley margin in several places, and at these locations the valley margin bank

consists of poorly sorted cobbly colluvium. These outcrops also are a source of gravel to the modern stream channel.

The modern stream channel is able to carry gravel up to 4.5 cm in b-axis diameter (pebble size) during high flow events, as determined from painted gravel tracer studies by students in the Geomorphology class during field experiments in the fall of 2009 (Figure 30). The high banks of the modern incised channel enable flow of sufficient depth to generate the shear stresses needed to transport pebbles, sand, and finer sediment during storms and snow melt events. The gravel tracer studies revealed that the pebble-sized gravel moves only during the largest events and only up to a few meters per event. Gravel that is larger than 4.5 cm (b-axis) has not moved since emplacement of the tracers at the study sites in the fall of 2009. Whereas this gravel moves as bedload, the finer sediment, including clay, silt, and fine to medium sand, moves as suspended load during storms.

DISCUSSION

The bank pin data yield the highest average annual erosion rates for bank Type 1a (ranging from -63.0 to -4.3 cm/yr, with an average of -23.9 cm/yr). Average annual erosion rates are slightly less for bank Type 1b (-30.7 to -31.4 cm/yr with an average of -31.1 cm/yr), and are lowest for bank Type 2. Bank Type 3 is characterized by net deposition (positive values). Deposition was measured at only two pin sites because bank advance buried the pins at other sites and prevented repeat measurement.

The data for both bank pins and cross sections show clearly that bank Types 1a and 1b have the highest rates of bank retreat (see Figure 27). Bank Type 2 yielded both some positive (deposition) and negative (erosion) values, but the average rates of change for both cross sections

and pins are close to zero. Finally, for bank Type 3 most of the data from the cross sections plots to the right of the zero line, showing that bank Type 3 is characterized overall by net positive change, or deposition.

Tables 9-12 show the total change in volume of sediment as calculated three different ways for erosion and one way for deposition. The different methods were explained previously in the "Calculations" section of this paper. Figure 31 provides a comparison of the annual mass of sediment (tons/yr) calculated with each method. This graph compares the tons of sediment for both deposition and erosion calculated in the previous graph. Erosion data from bank pins show much more spatial variability than do data from cross sections.

The cross sections show that no deposition has occurred on the high nearly planar surface adjacent to the stream channel. This feature represents the fill surface that formed during historic time, between the 18th and 20th centuries, as a result of sedimentation in the valley bottom during a period of upland soil erosion. The modern channel is incised into this fill surface and no longer deposits material on this surface. The lidar data, cross sections, and field measurements of bank height for bank Type 1a all indicate that the height of this surface decreases upstream, particularly upstream of the tributary confluence. These data are consistent with the observation that the fill thickness increases downstream. This increase in thickness is likely to be associated with a downstream grade control, such as a small dam, that promoted sedimentation on the valley bottom.

The results presented here are consistent with the findings of Wolman (1959), Lawler (1986), and Wynn et al (2008) with respect to the importance of freeze-thaw and needle ice in preparing the bank sediment for erosion. Substantial amounts of bank material were disaggregated throughout the study reach during the winter of 2009-10, particularly on bank

Types 1a and 1b. The weather data for this region showed that air temperature dropped below freezing at least 97 days during the winter of 2009-2010. Lawler (1986) determined that the number of days of freezing is the most important factor in rate of bank erosion for banks consisting of cohesive silt and clay.

The difference between erosion rates estimated from bank pins cross sections, the former of which are higher, might be due to several factors. First, the cross sections represent six years of change whereas the pins represent only one to two years. The cross sections are more likely to reflect an accurate long-term estimate for erosion. Second, the difference between erosion estimates from bank pins and cross sections probably reflects short-term temporal variability from season to season. The bank pin monitoring period included two winters and one summer for many of the pins and for the more recently installed pins only one fall and winter season. Both the short-term nature of the bank pin data, and the fact that the winter season is more heavily represented, might account for the high values of bank erosion from pin measurements (see Figure 27).

The provisional USGS gage station data (provided by Dr. Michael Langland) for water year 2009-2010 (October 2008 to September 2009) provides the following yields of total suspended sediment at the three gages:

1) The upstream gage on the western tributary yields 95 tons/yr;

2) the upstream gage on the eastern tributary yields 43 tons/yr; and

3) the downstream gage on the main stem yields 157 tons/yr.

The results of the stream bank study presented here indicate that as much as 111 to 144 tons/yr of sediment is deposited in the study reach between these gage stations. If so, then an amount equivalent to most, or even all, of the incoming 138 tons of sediment measured at the upstream gages might be deposited in the study reach. Accounting for this deposition, some 130 to 151 tons/yr of sediment must be eroded from the study reach in order to supply the 157 tons/yr measured at the downstream gage.

Based on cross sections re-surveyed after six years, the method thought to be the most representative of long-term average rates of erosion, as much as 175 to 227 tons/yr of erosion occurred within the study reach. These values are 58% higher than the estimated amount of deposition within the study reach, and 35-50% higher than the amount of erosion estimated for the study reach from gage station data. Possible causes of this difference are as follows. Much of the sediment eroded from banks might be in temporary storage in the study reach. However, we estimate an amount of storage for bank Type 3 based on rate of deposition along the inside of meander bends from the cross sections, and this amount accounts for the incoming load of sediment (95 + 43 = 138 tons/yr). Furthermore, grain-size data indicate that recently deposited sediment along bank Type 3 is coarser grained than sediment eroded from bank Types 1a and 1b; if so, then the predicted load of fine sediment from bank erosion is even higher than 30 to 139 tons (see Figure 31).

It is possible that additional sediment is in storage as large blocks that have calved or slumped from the banks. We noted many such blocks, particularly along bank Type 2. These blocks remain in the channel for up to several years, and the roots of grasses at the tops of these blocks help to maintain their strength for several years. In some places many slump blocks formed during large storms, particularly Hurricane Hannah in 2008 (observations during Fall

2008 Geomorphology class). Upstream of channel constrictions and grade controls, such as a bridge crossing with a culvert in the channel on the western tributary (see Figure 1), these large blocks have not been completely removed in the 1.5 years since Hurricane Hannah.

The erosion rates quantified during this investigation might be erroneously high because the sites chosen for cross sections had unusually high rates, or because the length of bank mapped as having such rates is too large. The first possible explanation is less likely, because 14 of the 19 bank pin sites had higher erosion rates than the average rate for the cross section sites for bank Types 1a and 1b. Bank erosion is highly variable spatially, however, and quantifying this variability is challenging. Nevertheless, estimates of erosion from pins, cross sections, and repeat digital orthophotos all support the conclusion that bank erosion is rapid along bank Types 1a and 1b. The length of each bank type was based on field mapping and subsequently confirmed by examination of repeat digital orthophotos. Each bank type is distinctive and the end points of mappable segments generally are fairly clear. It is possible, however, that the total length of bank Type 1a or 1b that was estimated to be eroding is higher than the actual length that actively did erode during the study period.

Both the error in measuring rates of erosion and deposition as well as the uncertainty in extrapolating these rates to estimate tons of sediment eroded or deposited over time are assessed here (Appendix 4). The error in measuring the pins, for example, is ±1 cm (2 cm in total), and this estimate is multiplied by bank height and unit length to get volume of sediment eroded. The error in measuring bank height is ±2 cm (4 cm in total), and the error in extrapolating this along a unit stream length on an irregular surface is also ±2 cm (4 cm in total). Assuming a plausible change scenario of 0.07 m^3 per year, the uncertainty in measurement of volume change over a period of one year with erosion pins is 14.6%. The error in measuring the cross sections is

assessed in the same way as for the pins. Assuming a plausible amount of change of 0.85 m^3 per year over the area of cross section, the uncertainty in measurement of volume change over a period of one to two years with cross sections is 25.8%.

This uncertainty would decrease with time for both methods, for two reasons. First, the relative proportion of measurement error to magnitude of change would decrease with time because the amount of change increases with time. Second, bank erosion and deposition are temporally and spatially variable, and years with more floods or freeze-thaw cycles, for example, might result in much greater amounts of change. As a result, the proportion of measurement error relative to magnitude of change would decrease with time. For both reasons the estimates of volume change from the cross sections are considered to have less uncertainty than those based on pin measurements. This conclusion is supported by the finding that the 12 cross sections yielded smaller standard deviation values for volume change than did the pins.

Error for stream flow and suspended flow estimates can be evaluated as follows (Allen Gellis, USGS, 2010, personal communication). The errors involved in making stream flow measurements include wind, boundary conditions, equipment, and measurement error (Sauer and Meyer, 1992). Most errors in stream flow measurements range from 3 to 6 % (Sauer and Meyer, 1992). During a runoff event the streambed may scour or fill and cause changes in the rating curve. These shifts in the streambed cannot be accurately quantified and are estimated by the persons analyzing the stream flow record. During the course of operation of a gaging station, the record may be incomplete as a result of power disruptions, adverse weather conditions, and vandalism, all of which will affect the final discharge computation. Suspended-sediment load computation may involve errors associated with collection, laboratory analysis, and records

computation. Similar to discharge computations, missing periods of sediment data will affect the final sediment data records computation.

CONCLUSIONS

This study supports the hypothesis that stream banks can be a major source of sediment from a stream that is incised into fine-grained historic sediment. The research presented here quantifies the load of suspended sediment from accelerated bank erosion after channel incision into fine-grained sediment. By determining rates of erosion and deposition within a stream reach that has monitoring data for both incoming and outgoing loads of suspended sediment, this study is able to determine how much of that load might be from bank erosion. The findings of this study indicate that all of the suspended sediment load measured at the downstream gage could be from stream bank erosion.

The stream bank material at BSR, mostly silt and clay, is prone to erosion by subaerial processes, particularly freeze-thaw and needle ice formation during the months of December through March. Bank pin data indicate high rates of erosion during the winter season. However, the actual entrainment of sediment and its subsequent downstream transport appear to be associated with high flow events. This conclusion is consistent with USGS gage data provided by M. Langland, which shows that the majority of suspended sediment transport occurs during the months of April through August.

Recently, Walter and Merritts (2008) determined that stream bank erosion in the mid-Atlantic region is likely to be greater at present than prior to European settlement because fine-grained sediment stored in millponds upstream of 18th to early 20th c. dams is prone to erosion as aging milldams breach. After dam breaching, stream channels become incised, forming high

banks in historic reservoir sediment. Pizzutto and O'Neal (2009) tested this hypothesis on the South River, Virginia, and determined that mean bank erosion rates increased by at least two times after eight milldams breached in the mid-20th c. The results presented here further support the hypothesis that stream bank erosion rates are high subsequent to channel incision, and in the case of BSR are sufficiently high to account for the entire measured suspended sediment load.

ACKNOWLEDGEMENTS

There were many people who helped me during the course of my thesis and I would like to take this opportunity to thank them. Many thanks to: Mike Rahnis for his help in the field, on the computer, and with a few of the figures; Cheryl Shenk for providing the beautiful photographs of BSR for which I am most grateful as well as for compiling the stunning panoramic images; Laura Kratz and Stacey Sosenko for analyzing soil samples; the geomorphology classes of '08-'09 for setting up the tracer gravel experiment; the USGS for providing data on BSR and Mike Langland in particular for calculating the provisional results of total mass of suspended sediment for the '08-'09 water year; my Thesis Honors Committee consisting of Dr. Roger Thomas, Dr. Andy DeWet, and Dr. Allen Gellis; the land owners of BSR, Joe Sweeney and Harlan Keener; the Committee on Grants for assisting in the purchase of the HOBO data sensor; and Dr. Bob Walter for sharing his input, insight, and experience.

Special thanks go to my advisor, Dr. Dorothy Merritts, who helped me in so many ways; I doubt I can recall them all. Dr. Merritts taught me how to conduct research in the field, the ways of looking at and analyzing data, and how to write more scientifically. Her perpetual enthusiasm motivated me to build a strong thesis. Without her guidance and vast knowledge of the topic this would not have been possible.

Final thanks go to my mother, Dave, and all my friends for their continual support throughout this project.

REFERENCES

Allmendinger, Nicholas E., James E. Pizzuto, Glenn E. Moglen, and Mikolaj Lewicki. 2007. A Sediment Budget for an Urbanizing Watershed, 1951-1996, Montgomery County, Maryland, U.S.A. *Journal of the American Water Resources Association* 43, no. 6 (December): 1483-1498. doi:10.1111/j.1752-1688.2007.00122.x.

Blackmer, Gale C. 2007. *Bedrock Geologic Map of the Quarryville and Conestoga Quadrangles, Lancaster County, Pennsylvania*. Open File Report. 4th Series. Harrisburg, PA: Pennsylvania Geological Survey. http://www.dcnr.state.pa.us/topogeo/openfile/conquarry.pdf.

Couper, Pauline. 2003. Effects of silt-clay content on the susceptibility of river banks to subaerial erosion. *Geomorphology* 56, no. 1-2 (November 15): 95-108. doi:10.1016/S0169-555X(03)00048-5.

Dietrich, William E., Thomas Dunne, Neil F. Humphrey, and Leslie M. Reid. 1982. Construction of Sediment Budgets for Drainage basins. In *Sediment Budgets and Routing in Forested Drainage Basins: Proceedings of the Symposium*, ed. Frederick J. Swanson, Richard J. Janda, Thomas Dunne, and Douglas N. Swanston, 5-23. General Technical Report PNW-141. Corvallis, OR: Pacific Northwest Forest and Range Experiment Station, Forest Service, U.S. Department of Agriculture. http://www.treesearch.fs.fed.us/pubs/7749.

Galeone, Daniel G., Robin A. Brightbill, Dennis J. Low, and David L. O'Brien. 2006. *Effects of streambank fencing of pasture land on benthic macroinvertebrates and the quality of surface water and shallow ground water in the Big Spring Run basin of Mill Creek watershed, Lancaster County, Pennsylvania, 1993-2001*. Scientific Investigations Report 2006-5141. Reston, VA; Denver, CO: U.S. Dept. of the Interior, U.S. Geological Survey. http://pubs.er.usgs.gov/usgspubs/sir/sir20065141.

Gellis, Allen C., William S. L. Banks, Michael J. Langland, and Sarah K. Martucci. 2004. *Summary of suspended-sediment data for streams draining the Chesapeake Bay Watershed, water years 1952-2002*. Scientific Investigations Report. Washington D.C.: U.S. Department of the Interior, U.S. Geological Survey. http://pubs.er.usgs.gov/usgspubs/sir/sir20045056.

Lawler, D. M. 1986. River Bank Erosion and the Influence of Frost: A Statistical Examination. *Transactions of the Institute of British Geographers* 11, no. 2. New Series: 227-242. doi:10.2307/622008.

———. 1988. Environmental Limits of Needle Ice: A Global Survey. *Arctic and Alpine Research* 20, no. 2 (May): 137-159. doi:10.2307/1551494.

Lawler, D. M., C. R. Thorne, and J. M. Hooke. 1997. Bank erosion and instability. In *Applied Fluvial Geomorphology for River Engineering and Management*, ed. C. R. Thorne, R. D. Hey, and M. D. Newson, 137-172. Chichester: Wiley.

Lawler, D.M. 1993. Needle ice processes and sediment mobilization on river banks: the River Ilston, West Glamorgan, UK. *Journal of Hydrology* 150, no. 1 (September): 81-114. doi:10.1016/0022-1694(93)90157-5.

Outcalt, Sam I. 1971. An Algorithm for Needle Ice Growth. *Water Resources Research* 7, no. 2: 394-400. doi:197110.1029/WR007i002p00394.

Pizzuto, Jim, and Michael O'Neal. 2009. Increased mid-twentieth century riverbank erosion rates related to the demise of mill dams, South River, Virginia. *Geology* 37, no. 1 (January): 19-22. doi:10.1130/G25207A.1.

Simon, Andrew, Andrea Curini, Stephen E. Darby, and Eddy J. Langendoen. 2000. Bank and near-bank processes in an incised channel. *Geomorphology* 35, no. 3-4 (November): 193-217. doi:10.1016/S0169-555X(00)00036-2.

Snyder, Noah P., Michael R. Castele, and Jed R. Wright. 2009. Bedload entrainment in low-gradient paraglacial coastal rivers of Maine, U.S.A.: Implications for habitat restoration. *Geomorphology* 103, no. 3 (February 1): 430-446. doi:10.1016/j.geomorph.2008.07.013.

Sullivan, Alexandra (F&M 2006), Geomorphology in the agricultural watershed of Big Spring Run (Lancaster, PA): An integrative approach to erosion research and remediation: Undergraduate senior thesis, Department of Earth and Environment, 51 p.

Voli, Mark, Dorothy Merritts, Robert Walter, Erik Ohlson, Katherine Datin, Michael Rahnis, Laura Kratz, Wanlin Deng, William Hilgartner, and Jeffrey Hartranft. 2009. Preliminary Reconstruction of a Pre-European Settlement Valley Bottom Wetland, Southeastern Pennsylvania. *Water Resources Impact* 11, no. 5 (September): 11-12.

Walter, R.C., & Merritts, D.J. (2008). Natural Streams and the Legacy of Water-Powered Mills. *Science*,319 (5861), 299-304.

Washburn, A. L. 1979. *Geocryology: A survey of periglacial processes and environments*. London: E. Arnold.

Wolman, M. Gordon. 1959. Factors influencing erosion of a cohesive river bank. *American Journal of Science* 257, no. 3 (March): 204-216.

Wynn, T.M., M.B. Henderson, and D.H. Vaughan. 2008. Changes in streambank erodibility and critical shear stress due to subaerial processes along a headwater stream, southwestern Virginia, USA. *Geomorphology* 97, no. 3-4 (May 15): 260-273. doi:10.1016/j.geomorph.2007.08.010.

FIGURES LIST

Figure 1. Map of Big Spring Run...38
Table 1. Weather data for Lancaster county..39
Figure 2. Topographic map of BSR showing gage station location...40
Figure 3. Elevation map of BSR with hillshade relief..41
Table 2. Definition of terms...42
Table 3. Influential factors in bank erosion systems..42
Figure 4. Diagram of subaerial processes and sediment transfer in cohesive banks..43
Figure 5. Graph showing erodibility increasing with silt-clay content..43
Figure 6. Photograph of needle ice..44
Figure 7. Illustration showing needle ice and sediment transfer...45
Figure 8. Digital orthoimage showing pin location for entire stretch of BSR...46
Figure 9. Digital orthoimage showing pin location for high pin density section of BSR...46
Figure 10. Digital orthoimage showing the location of "Houser Grid Site"..47
Figure 11. Digital orthoimage showing locations of cross sections..48
Figure 12. Photographs of the four bank types..49
Figure 13. Illustration of the procedure for calculating area of erosion and deposition from cross sections..50
Figure 14. Photo of HOBO sensor placement and map showing location..51
Figure 15. Digital orthoimage showing bank type mapping..52
Table 4. Length and height of bank types and total length..53
Figure 16. Lidar with digital orthoimage drapped on top showing bank Types 1a and 1b.....54
Figure 17. Lidar with digital orthoimage drapped on top showing bank Type 3..55
Figure 18. Image showing mass movement...56
Figure 19. Image showing partial bank collapse...56
Figure 20. Images of slump block at "Type Locality"..57
Figure 21. Images of needle ice causing bank erosion..58
Figure 22. Image showing needle ice apron and sediment erosion due to fluvial entrainment..59
Figure 23. Freeze-thaw events captured with HOBO sensors...60
Figure 24. Comparison of orthoimages from 2001, 2005, and 2008..61
Figure 25. Aerial photograph of "Type Locality"(May, 2007) current bank location shown 62
Figure 26. Aerial photographs from 2007 showing abandoned bend in BSR...63
Table 5. Average rate of change for each set of pins..64
Table 6. Data for all 12 cross sections...65
Table 7. Rate of retreat and advance from cross sections..66
Table 8. Comparison of rate of retreat and advance from pins and cross sections..67
Figure 27. Graphs comparing rates of change for pins and cross sections for all bank types.....68
Figure 28. Map showing sediment sample collection sites..69
Figure 29. Ternary soil texture diagram for percent sand, silt, and clay by mass..70
Figure 30. Gravel clasts that moved during high flow events and map showing location.....71
Tables 9-12. Different methods of calculating erosion and deposition and results...72
Figure 31. Comparison of average tons of sediment eroded or deposited..73
Appendix 1. Cross section survey methodology..74

Appendix 2. Additional height information……..75
Appendix 3. 12 cross sections measured in 2004 and 2010…….76
Appendix 4. Table of methodological error……..82

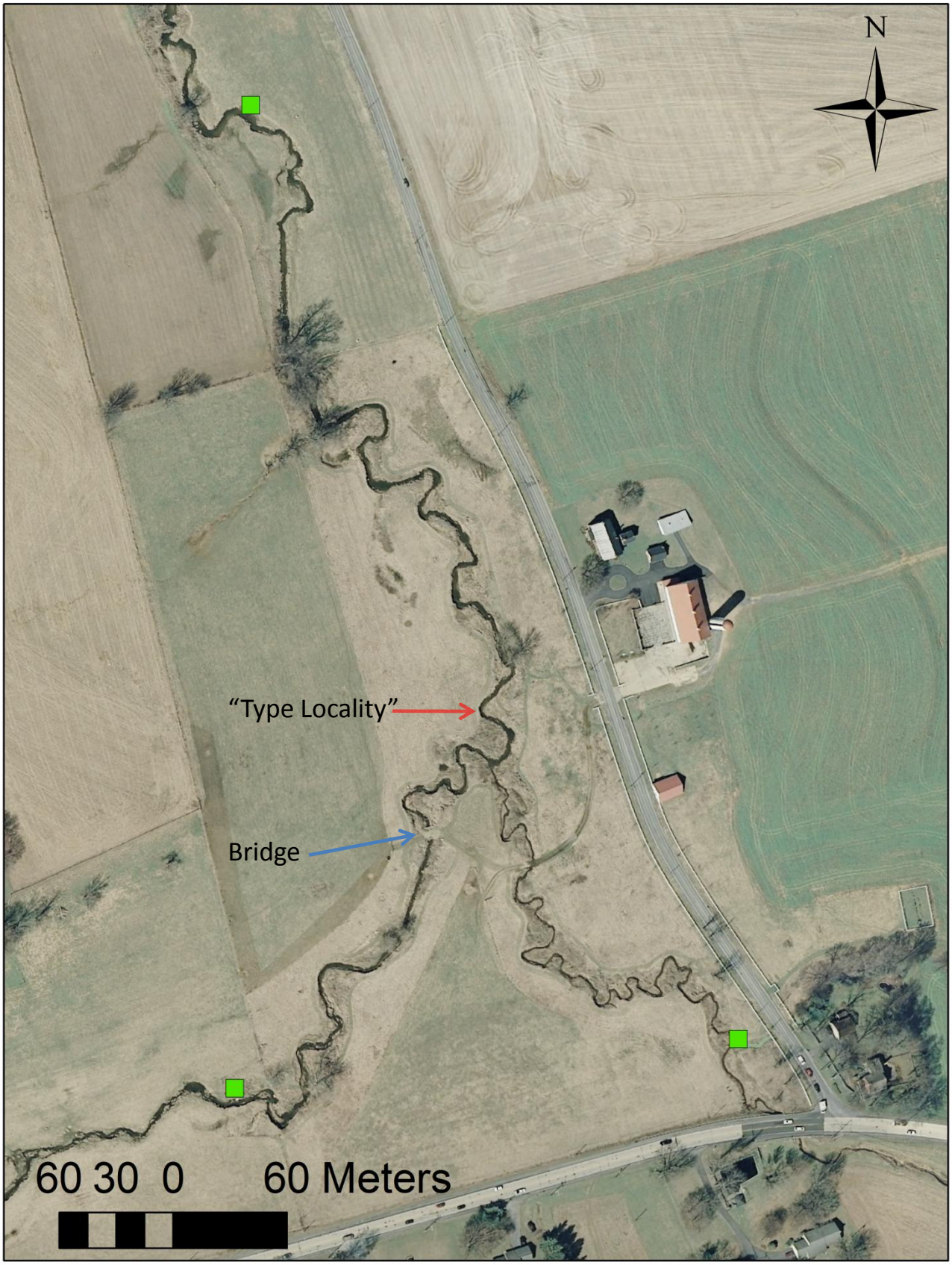

Figure 1. BSR study reach with the three U.S.G.S. gage stations, represented by green squares, collecting continuous data on water level, temperature, and turbidity.

Month	Average Temperature °F	Total Precipitation (inches)	Snow (inches)	High[1]	Low[2]
2009					
January	26.8	1.77	7.7	14	30
February	35.8	0.33	2.1	3	22
March	41.9	1.64	6.5	2	13
April	53.7	4.31	0	0	3
May	63	4.83			
June	70.4	5.25			
July	72.5	22.28			
August	75.3	8.23			
September	65	5.56			
October	53.8	5.78			
November	48.2	2.04	0	0	6
December	33.7	5.55	20.2	5	26
Average	**53.5**				
Total		**65.8**	**36.5**	**24**	**100**
2010					
January	31	1.66	1.2	11	29
February	30.7	3.4	50.3	5	25
March	47.5	3.13	0	0	11
Total to Date		**8.19**	**51.5**	**16**	**65**

Table 1. Weather data for the Lancaster/Millersville area from Millersville University Weather Information Center. http://www.atmos.millersville.edu/~cws/climo/monthly-data.html (date accessed: 4/17/10). [1]Days when both the high and low temperatures for the day were at or below 32° F. [2]Days when the low temperature for the day was at or below 32° F.

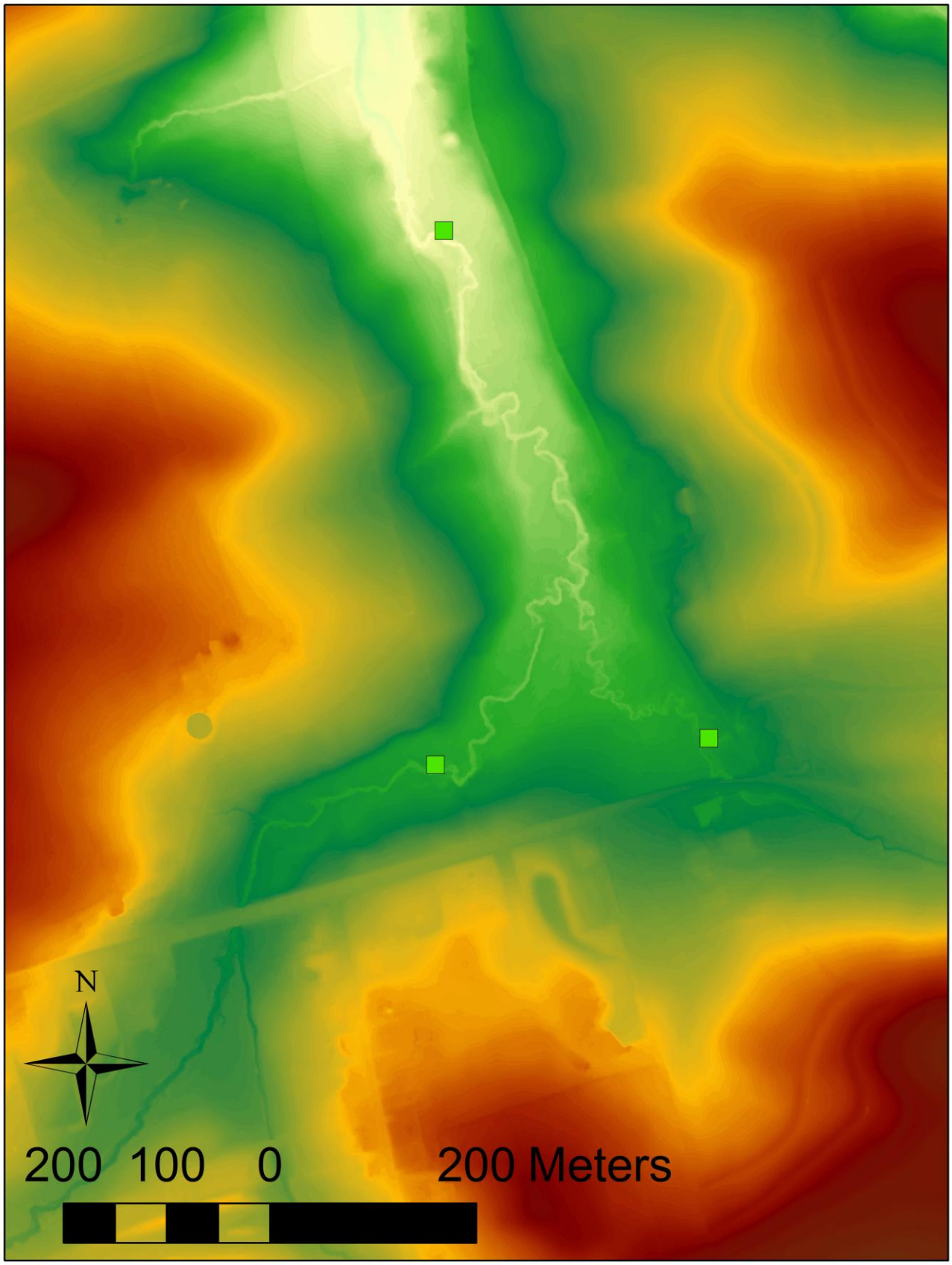

Figure 2. Topographic map generated from lidar elevation data for BSR study reach. Green squares show locations of the three U.S.G.S. gage stations. The highest elevation, in deep red, is 122 m; lowest elevation along channel near northernmost gage station, in pale green, is 92 m.

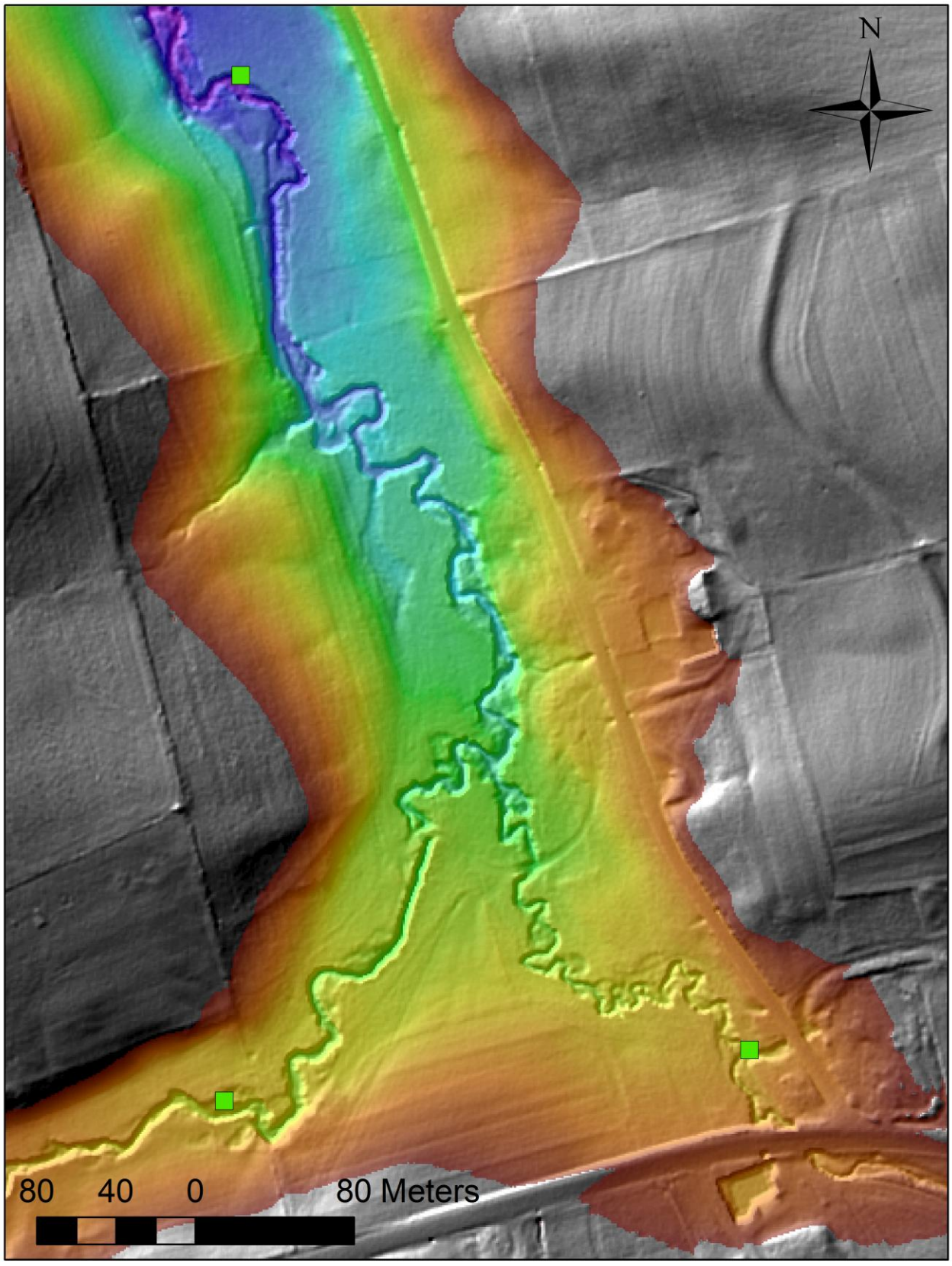

Figure 3. Elevation data from 2008 lidar for the valley bottom draped above hill shade relief.

Definition of terms

Bank erosion

Detachment, entrainment and removal of bank material as individual grains or aggregates by fluvial and subaerial processes

Bank failure

Collapse of all or part of the bank *en masse*, in response to geotechnical instability processes

Bank retreat

Net linear recession of bank as a result of erosion and/or failure

Bank advance

The opposite of bank retreat, i.e. net linear streamwise change in bank surface position, as a result of deposition of sediment or *in situ* swelling of bank materials

Bank erodibility

The ease with which bank material particles and aggregates can be detached, entrained and removed (normally by flow processes)

Table 2. Adapted from Lawler et al, 1997 Box 6.1.

Subaerial processes:

- freeze-thaw
- Dessication

Mass failure:

- Slumping
- Calving
- Toppling

Fluvial processes:

- Abrasion
- Plucking
- Bed load transport (ripples, bars)
- Suspended load transport (turbidity)

Table 3. Examples of erosion processes.

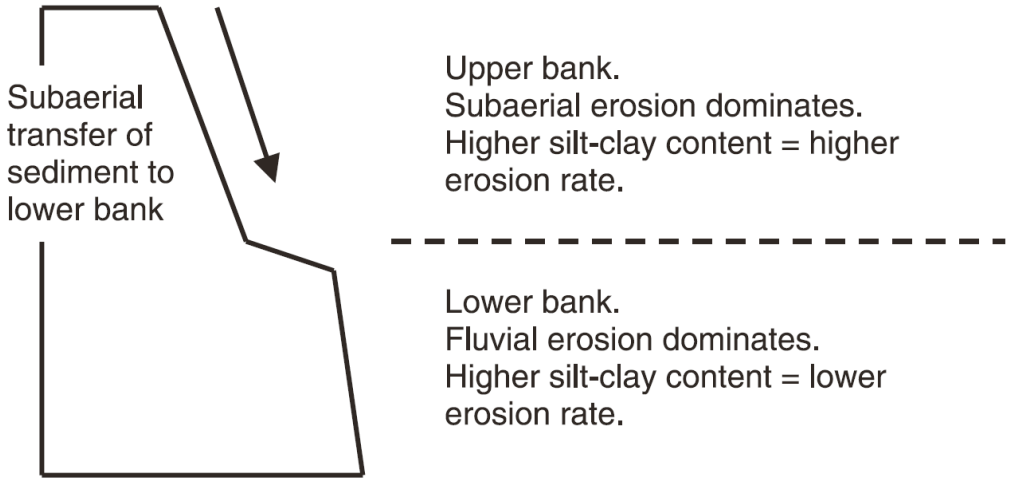

Figure 4. Diagram showing how subaerial processes aid in the transfer and erosion of sediment in cohesive banks (those with high silt-clay content). Adapted from Couper (2003) Figure 8.

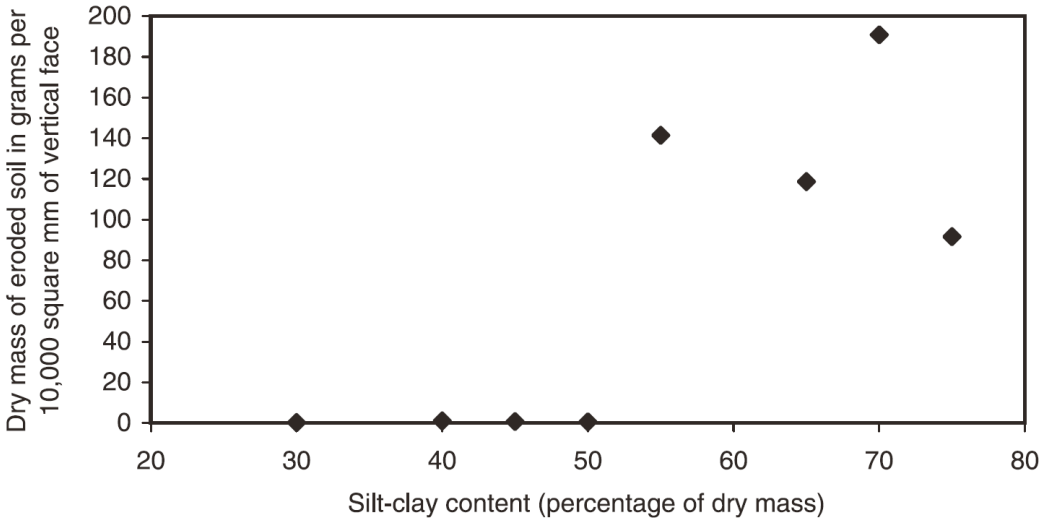

Figure 5. Graph showing how erodability increases with silt-clay content. Adapted from Couper (2003) Figure 5.

Figure 6. Photograph of needle ice removed from the banks of BSR. Metric ruler for scale.

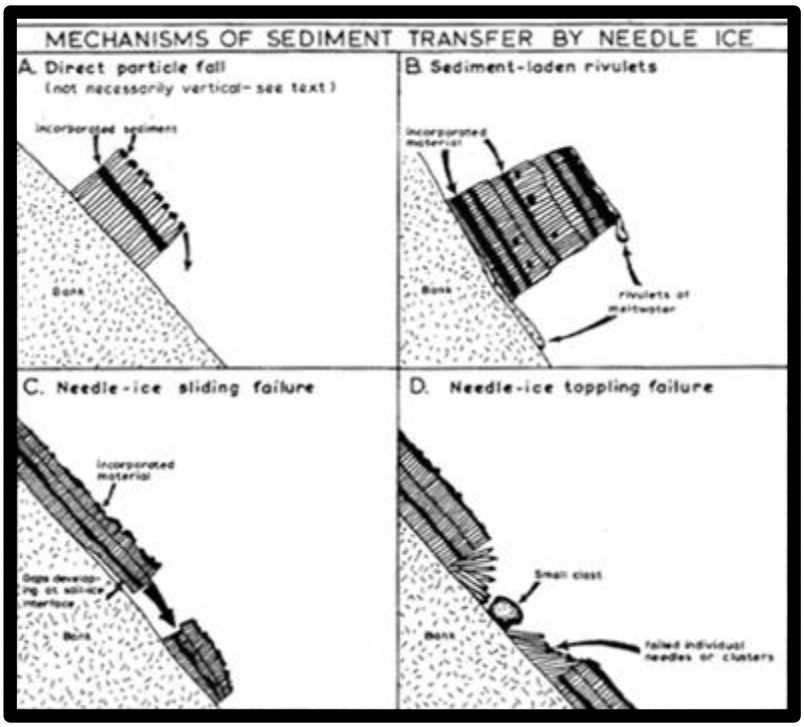

Figure 7. Illustration showing mechanisms of sediment transfer by needle ice. Adapted from Lawler et al, 1997.

Figures 8 & 9. Digital orthoimage (2008) showing the placement and identification of erosion pins along BSR. Inset photo below shows area of dense pins. Location of inset photo is shown as red box at right.

Figure 10. Digital orthoimage showing the location of the "Houser Grid Site" in relation to the BSR study reach. Location indicated by a red arrow.

Figure 11. Digital orthoimage (2008) showing the location of cross sections surveyed in 2004 and 2010.

Figure 12. Photographs of the four different bank types. Upper Left: Type 1a, bank height is 1.1 m. Upper Right: Type 1b, bank height is 0.9 m. Lower Left: Type 2, bank height is approximately 1 m. Lower Right: Type 3 indicated by a yellow arrow. Type 1b indicated by a blue arrow. Stadia rod on Type 3 bank edge is extended 2 m.

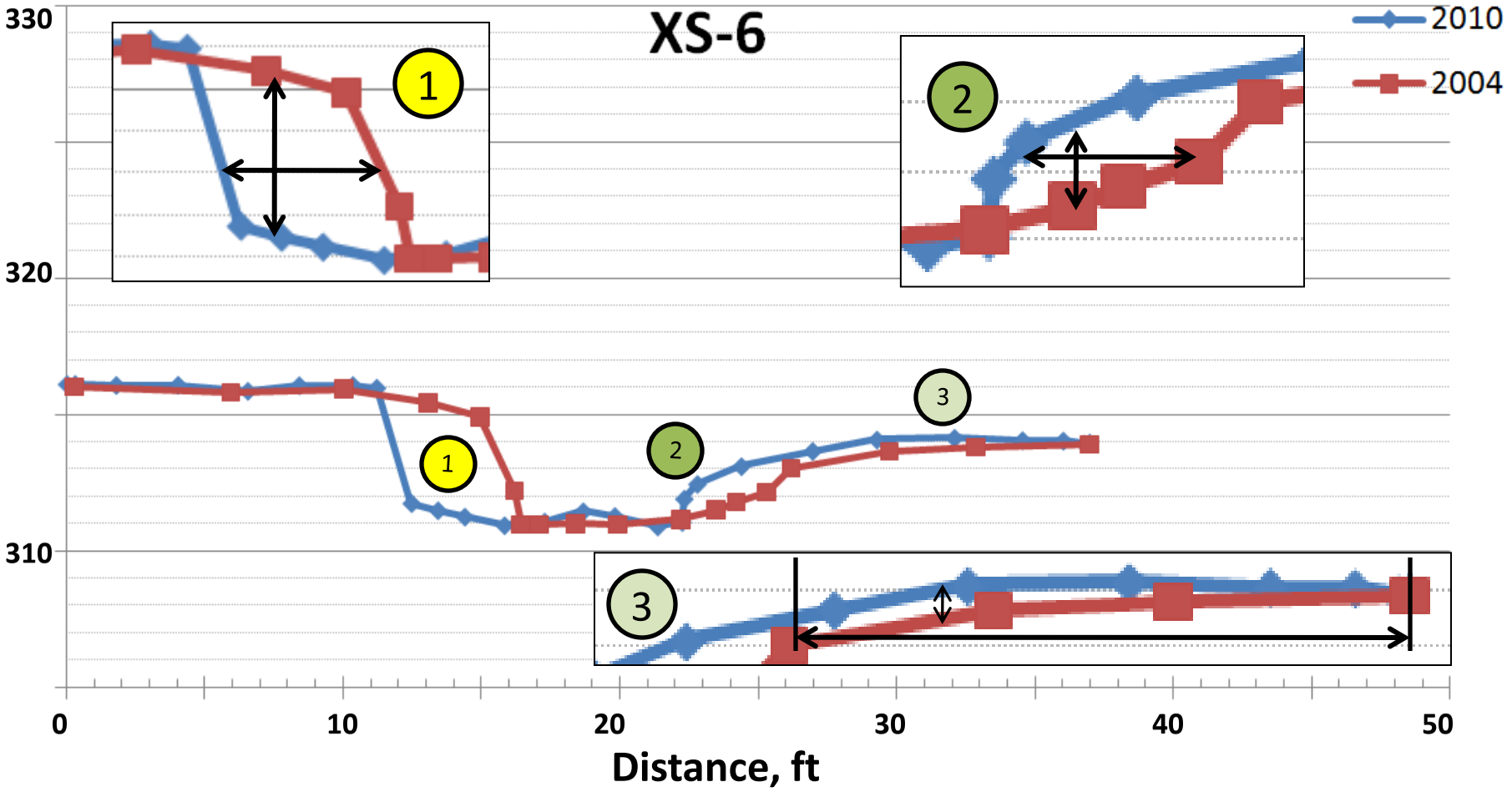

Fig. 13. Procedure for calculating area of erosion and deposition from repeat surveys of a stream channel cross section. In this example (cross section 6 at the "Type Locality"), left bank (as viewed downstream) is mapped as Type 1a and right bank as Type 3. In step (1), the average height (h) is measured and multiplied by the average width (w) to generate area. The area of deposition (2 and 3) is measured in the same manner. Deposition at the toe of the bank is shown as (2), and deposition at the top of the bank is shown as (3). For both erosion and deposition, the average area for all cross sections is calculated. This average value is multiplied by total bank length for the respective bank type in order to calculate volume of sediment eroded or deposited.

Figure 14. In the photo above the HOBO data logger is marked with a red arrow. It was placed high up on the bank to protect it from high flows and attached to a post to keep it safe. The sensors were placed at varying heights in the bank below, circled in yellow. The map to the left shows the location of the sensor (yellow dot) just north of the "Type Locality."

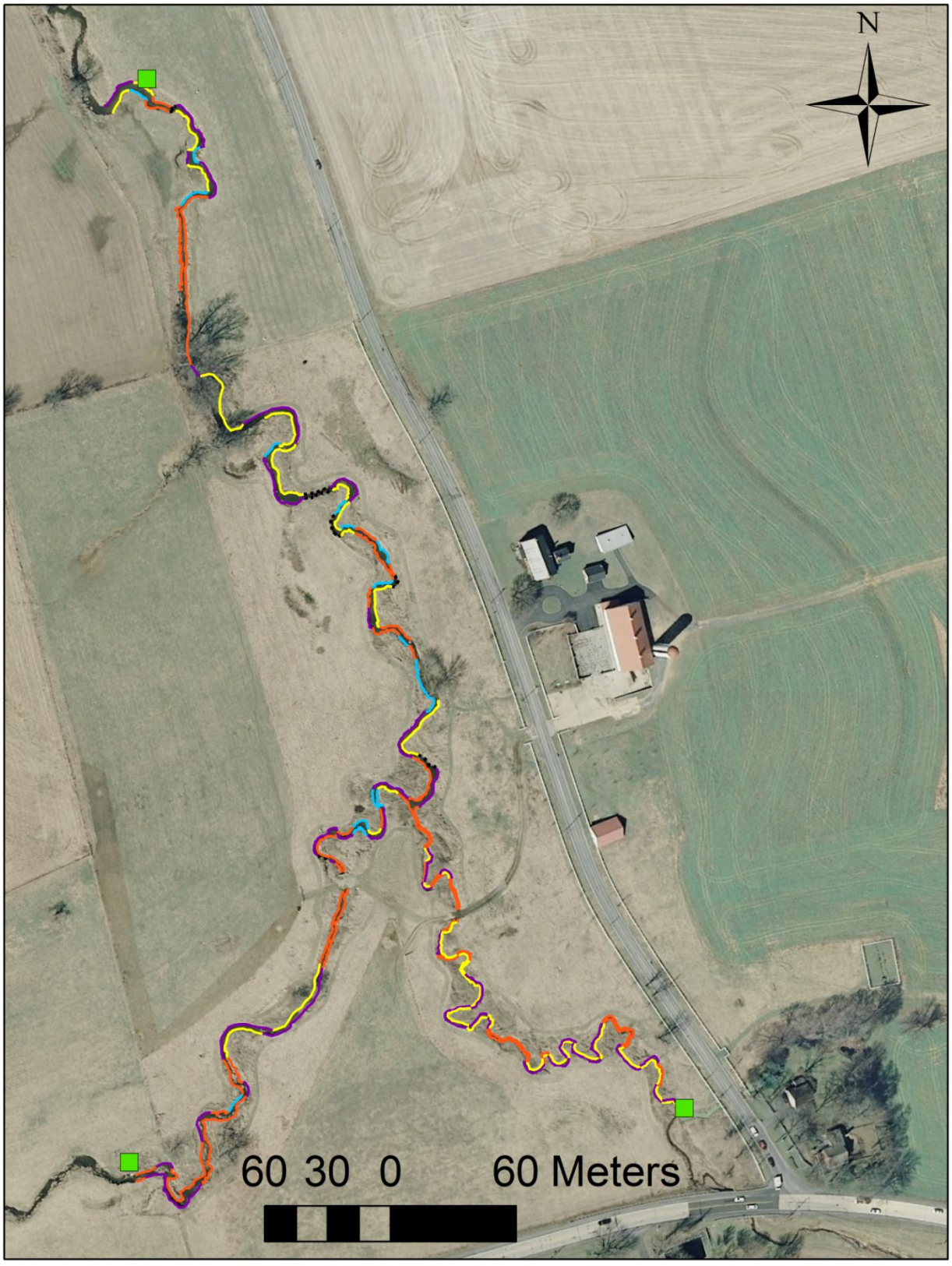

Figure 15. Digital orthoimage (2008) showing bank types. Purple represents Type 1a, blue Type 1b, orange Type 2, and yellow Type 3. Dashed black lines represent regions of rubble, originally laid down to protect a sewer line. Two segments of bank have been left uncolored. These banks are against the valley wall, which consists of colluvium and bedrock. The segments of bank downstream of the northernmost gage station have been mapped but were not included in the calculations.

Bank Type	**Total Bank Length** (m)	**Average Bank Height** (m)
1a	765	1.2
1b	187	1.1
2	994	1.0
3	671	na
Rubble	74	na
Colluvium	134	na
Total	2725	

Table 4. Total length of each type of bank and the average height for that type. Note that total bank length represents both left and right banks of stream channel, and is twice the actual channel length.

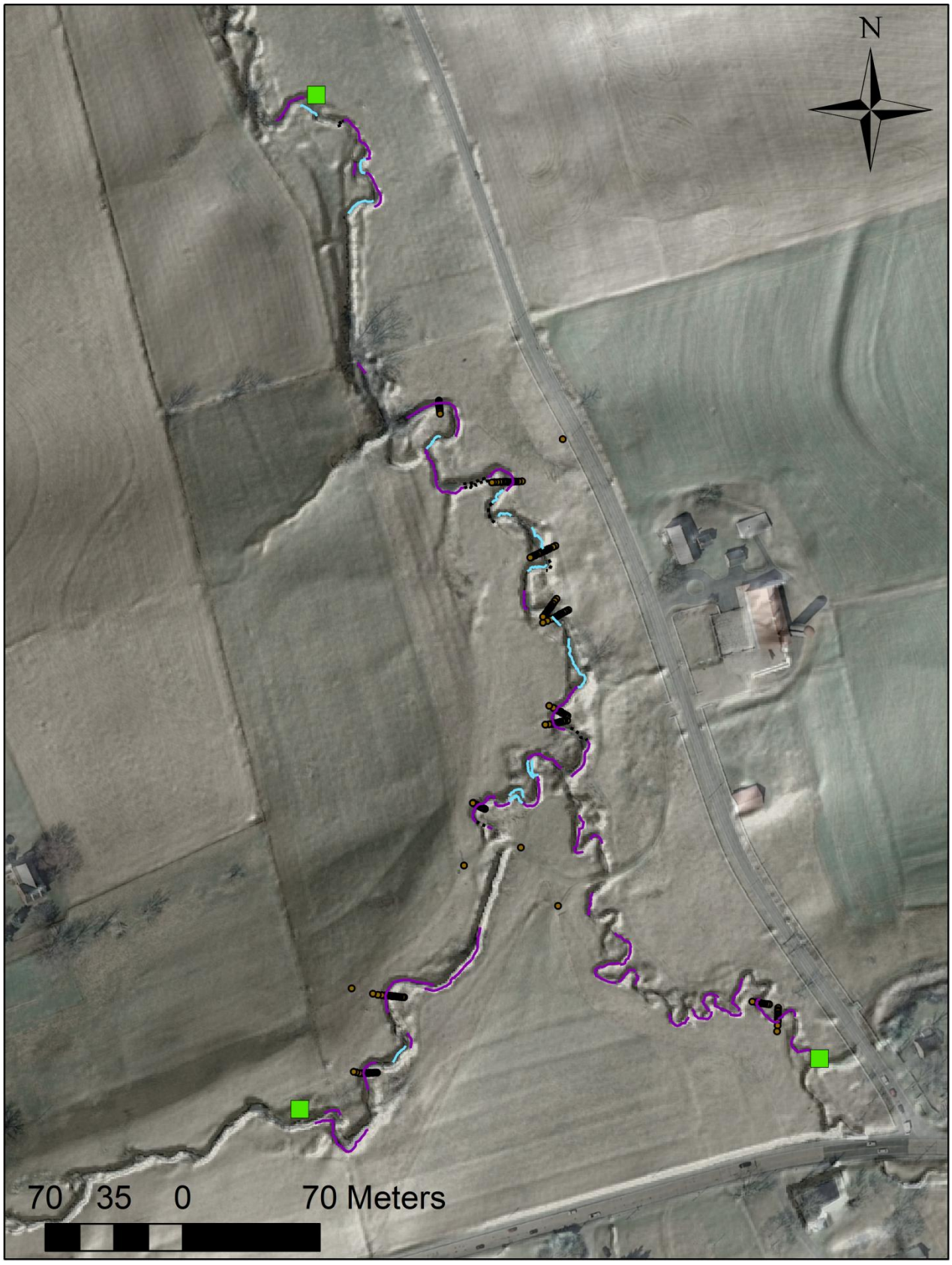

Figure 16. Lidar with 2008 digital orthophoto draped over top showing banks experiencing erosion (Type 1a in purple and Type 1b in blue). Total distance of Type 1a and 1b is 952 m.

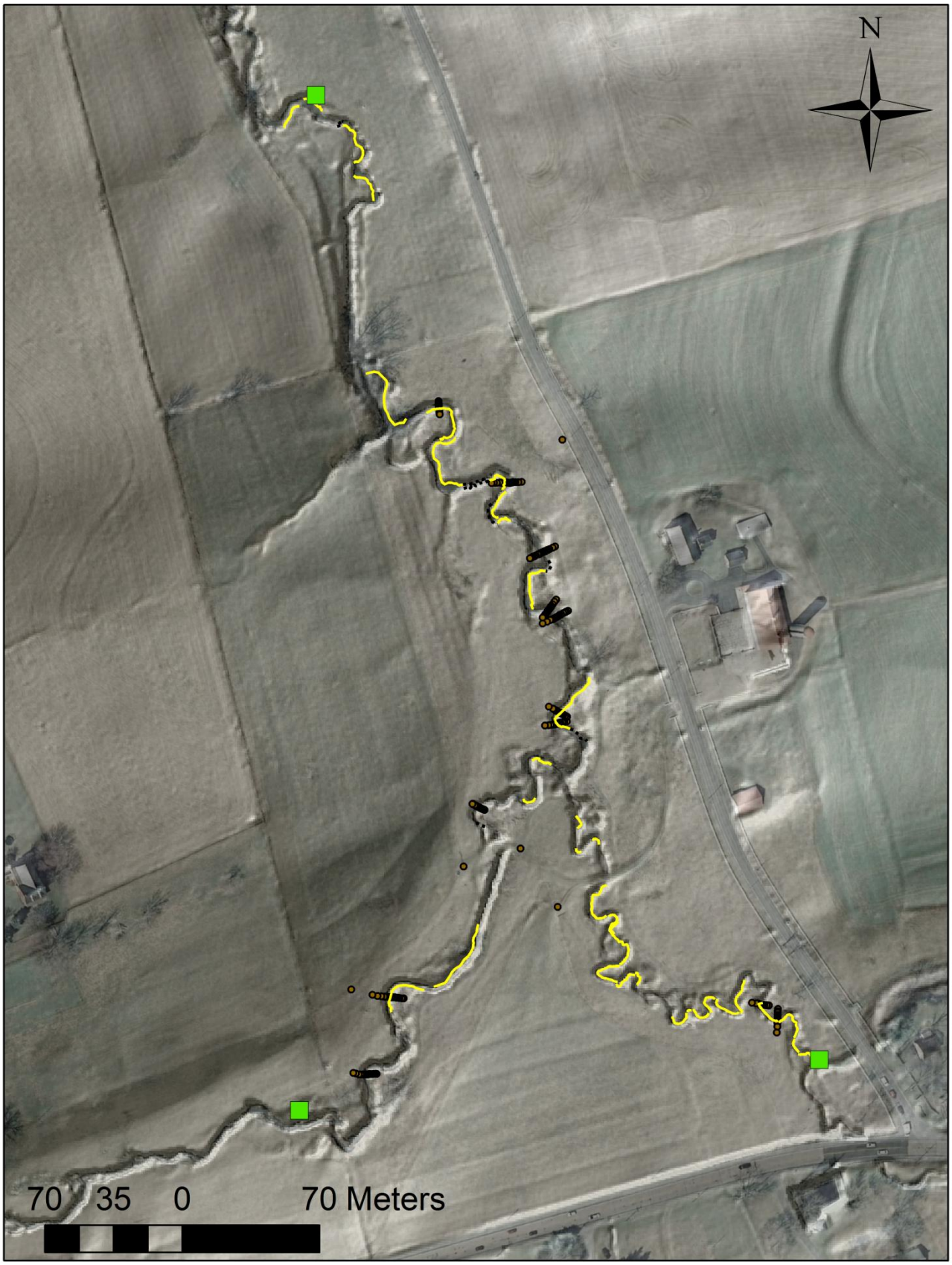

Figure 17. Lidar image with 2008 digital orthophoto draped over top showing banks experiencing deposition, Type 3 shown in yellow. Total distance of Type 3 banks 671 m.

Figure 18. (Above) Image showing mass movement erosion of a bank along BSR.

Figure 19. (Right) Image showing mass movement on a smaller scale, only part of the bank has collapsed.

Figure 20. Panorama photo showing the "Type Locality" after mass movement erosion. After an especially high flow even a large slump block fell into the stream as well as a tree which collapsed into the stream. The slump block is shown in an enlarged photo so that additional details of the mass movement can be seen. A red arrow in the panoramic photo indicates where the slump block was before it fell into the stream. The fallen tree is identified by a blue arrow.

Figure 21. (Above) image (taken 12/17/09) of a Type 1a bank showing needle ice formation and the layer of sediment pushed out ahead of the needle ice. Areas of sediment that have fallen into the water recently are obvious by the absence of moss. (Left) Image from the same day showing an apron of sediment collecting at the base of the bank below the needle ice.

Figure 22. Image showing both the formation of an apron of sediment at the base of the bank due to needle ice and the formation of a notch fluvial entrainment removed sediment from the base of the apron during a high flow event. Location of site is eastern tributary (UTM coordinates) 392857.867, 4427237.289).

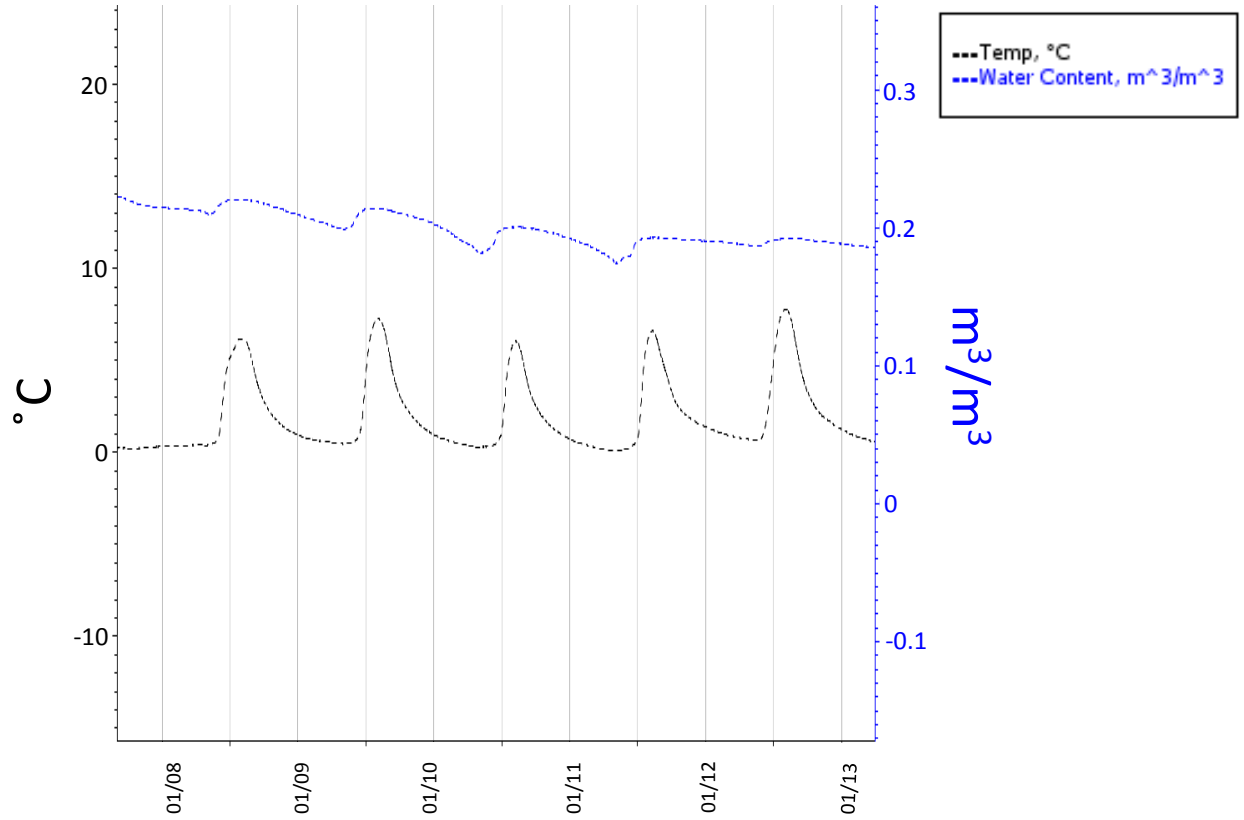

Figure 23. Five freeze-thaw events detected with two HOBO sensors placed in the stream bank at "Type Locality". Water content decreases with the lowering of temperature and formation of ice in the pore spaces of the bank sediment.

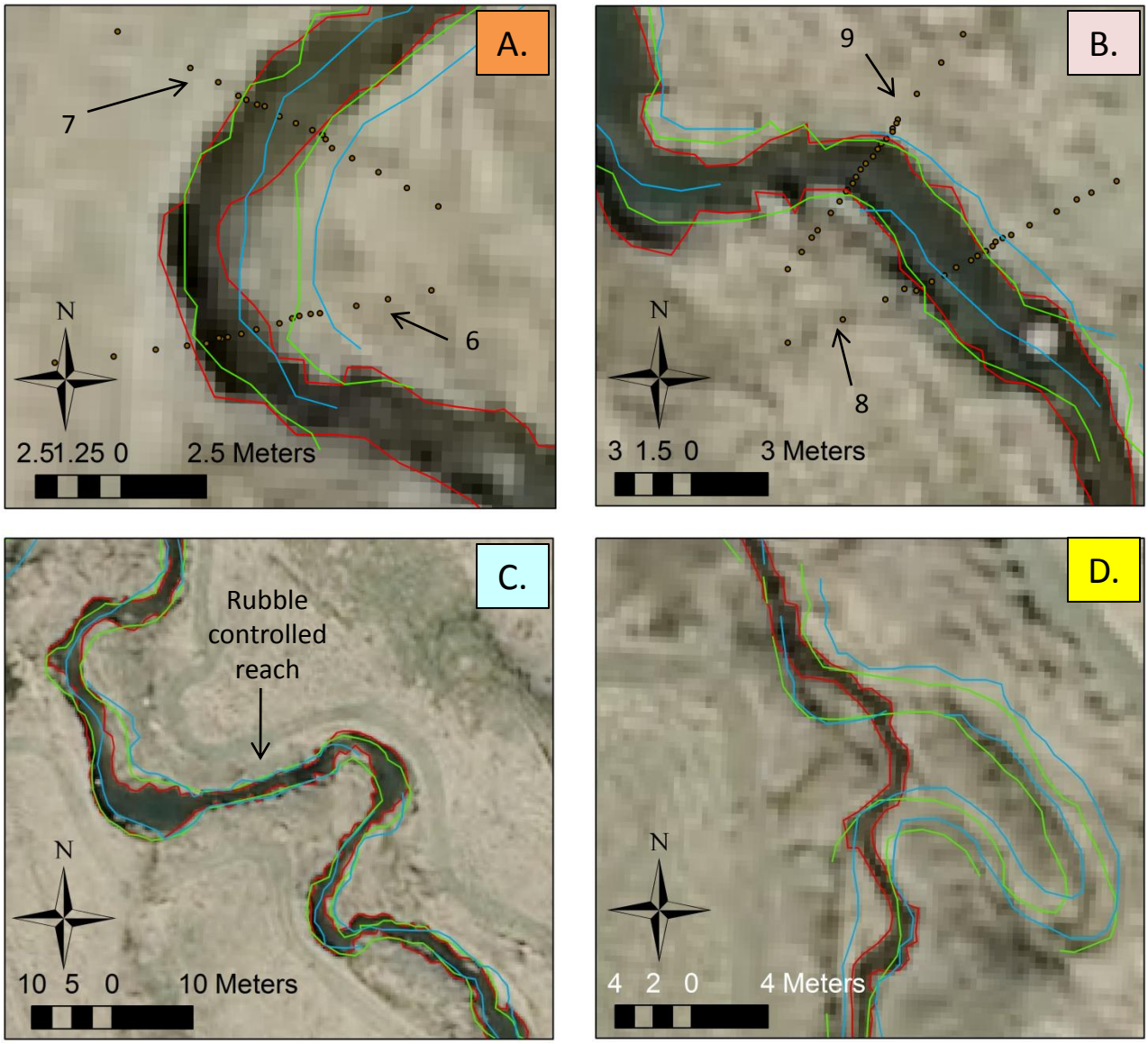

Figure 24. Four different views of BSR showing bank advance and retreat over 7 years. The blue lines represents the banks in 2001, green in 2005 and red in 2008. A.) "Type locality" with cross sections 6 and 7. B.) Cross sections 8 and 9. C.) Reach of BSR with rubble along banks, showing little channel movement during the 7 years. D.) A meander bend had cut off between 2005 and 2008. Map to the right shows the location of A, B, C and D (the four images above) using color coordinated dots along BSR. The color of the dots match the colors of the boxes with the letters for each image.

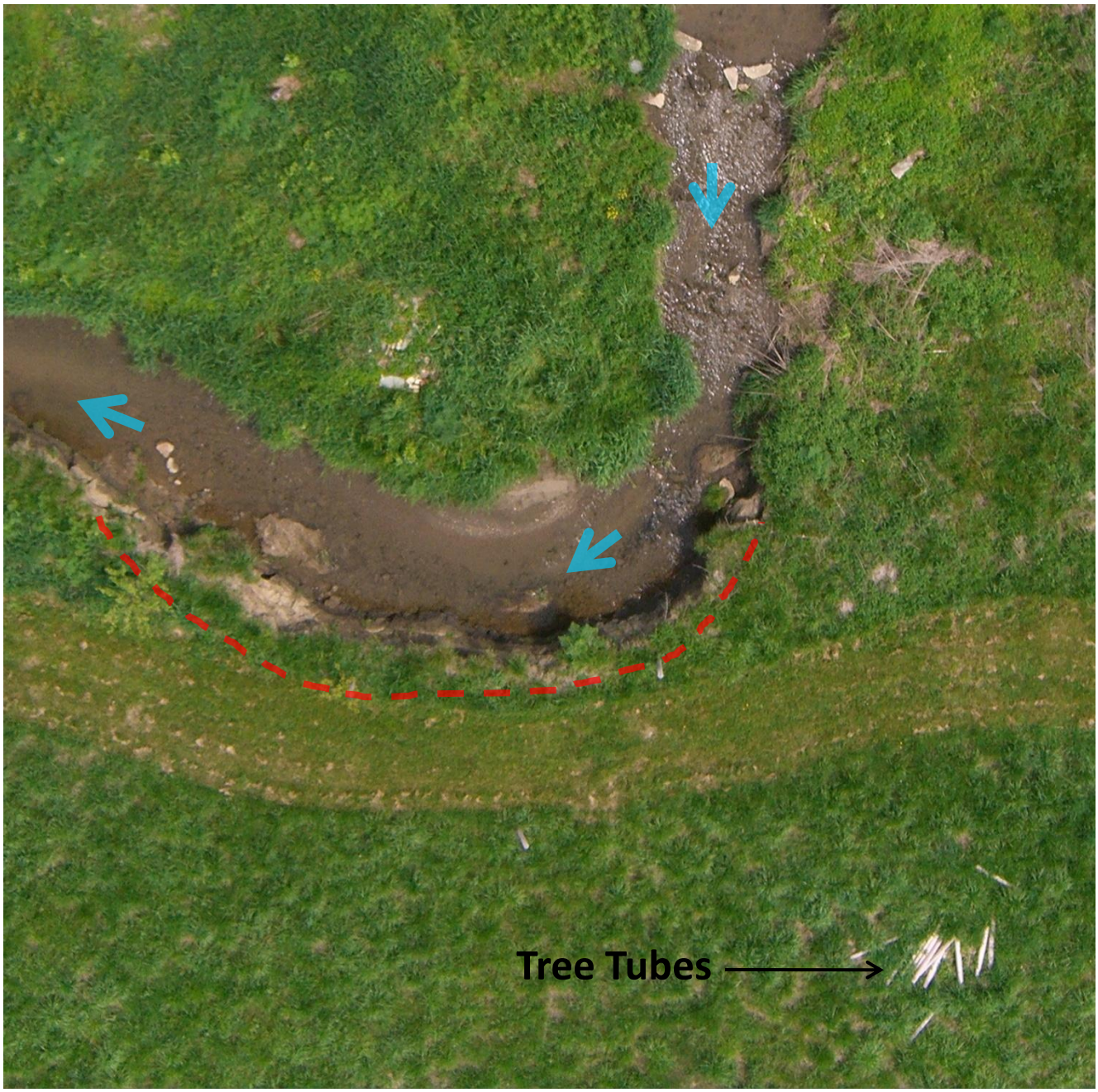

Figure 25. Aerial photograph of “Type Locality” in May, 2007. Dashed red line shows approximately where the bank is at present. Blue arrows designate water flow direction. Tree tubes are approximately 0.6 meters in length.

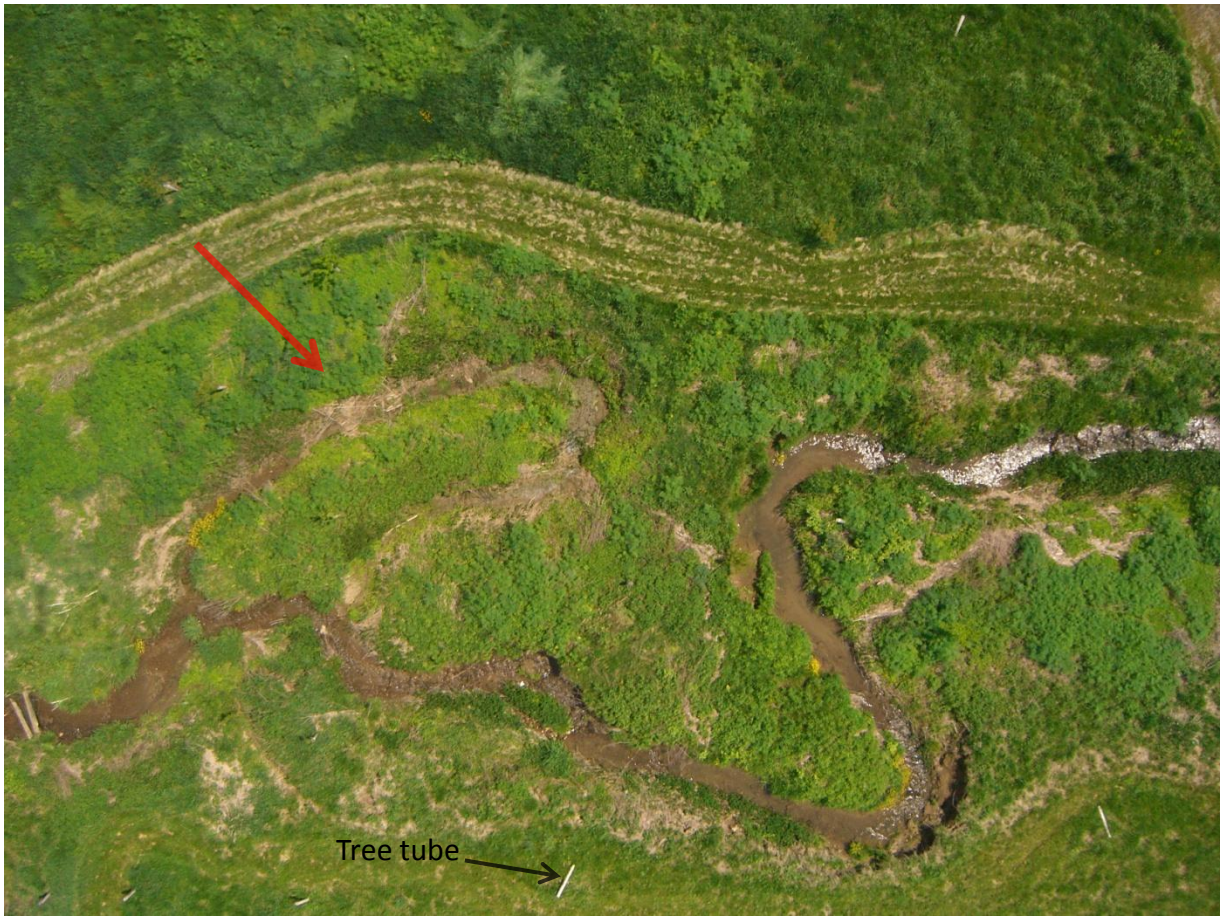

Figure 26. Aerial photos taken in 2007 showing and abandoned bend in BSR that was cut off between 2005 and 2008 as shown on image D in Figure 24. Red arrow points to the abandoned bend in each photo. Tree tubes are approximately 0.6 m in length. The manhole cover is approximately 0.7 m in diameter.

Bank Type	Pin Number	Rate of Change (cm/year)	Average Rate of Change (cm/year)
1a	78	-34.0	-23.9
1a	79	-27.7	
1a	80	-29.0	
1a	15	-17.3	
1a	14	-35.9	
1a	11	-10.0	
1a	10	-30.1	
1a	9	-14.4	
1a	68	-7.7	
1a	69	-43.1	
1a	70	-7.9	
1a	8	-63.0	
1a	7	-45.5	
1a	72	-25.4	
1a	5	-14.0	
1a	55	-4.3	
1a	56	-6.8	
1a	4	-18.8	
1a	57	-19.1	
1b	12	-30.7	-31.1
1b	62	-31.4	
2	63	0.6	2.2
2	64	-0.4	
2	66	-2.7	
2	1	7.7	
2	2	5.8	
3	13	4.4	8.5
3	6	12.6	

Table 5. Average rate of change for each set of pins (top, middle, and bottom pin) and in which bank type that set of pins is located. Negative values represent bank retreat (erosion) and positive values represent bank advance (deposition).

Cross Section	Bank Types	Bank Retreat (cm)	Bank Advance (cm)	Vertical Change (cm)	Retreat Rate (cm/year)	Advance Rate (cm/year)	Rate of Vertical Change (cm/year)
1	L3 R1a	R 96.0	L 6.1	L 14.3	R 16.0	L 1.0	L 2.4
2	L1a R3	L 81.7	R 87.2	R 11.9	L 13.6	R 14.5	R 2.0
3	L1a R2	L 49.1	R 56.1	R 10.4	L 8.2	R 9.4	R 1.7
4	L1a R3	L93.9	R 120.1	R 10.4	L 15.7	R 20.0	R 1.7
5	L1a R2	L*	R (insignificant)	R 0.4	L*	R (insignificant)	1.8
6	L1a R3	L 127.4	R 73.2	R 14.6	L 21.2	R 12.2	R 2.4
7	L1a R3	L 101.8	R 66.5	R 18.0	L 17.0	R 11.1	R 3.0
8	L2 R2	R 52.9	L 45.1	L 12.2	R 4.3	L 7.5	L 2.0
9	L2 R2	L 38.4 R 37.5	L 0.0 R 0.0	R 18.3	L 6.4 R 6.3	L 0.0 R 0.0	R 3.1
10	L2 R2	L 51.8	R 0.0	R 0.0	L 8.6	R 0.0	R 0.0
11	L3 R1a	L 78.0 R 52.1	L 0.0 R0.0	(insignificant)	L 13.0 R 8.7	R 16.1	(insignificant)
12	L3 R1a	R 79.9	L 94.1	L 13.1	R 13.3	L 15.7	L 2.2

Table 6. Data collected for 12 cross sections showing change from 2004 to 2010. See figure __ for location of each cross section, and Appendix ___ for graphs of the 2004 and 2010 surveys for each section. The 2004 surveys were done by Land Studies Inc. , surveyors.

Advance

Cross-Section	Bank	Bank Area (m^2)	Top Area (m^2)	Total Area per Bank (m^2)	Average Area (m^2)	Total Bank Length (m)	Volume deposited over 6 years (m^3)	Average Volume per year (m^3/ year)
1	Left	0.2	0.6	0.8	0.9	671.1	604.0	100.7
2	Right	0.6	0.4	1.0				
4	Right	0.8	0.5	1.3				
6	Right	0.6	0.5	1.1				
7	Right	0.4	1.1	1.5				
11	-	0	0	0				
12	Left	0.7	0.3	1.0				
Total		3.2	3.3	6.5				

Retreat

Cross-Section	Bank	Total Area per Bank (m^2)	Total Bank Area (m^2)	Average Area (m^2)	Total Bank Length (m)	Volume eroded over 6 years (m^3)	Average Volume per year (m^3/ year)
1	Right	0.5	8.6	1.0	952.2	952.2	158.7
2	Left	0.5					
3	Left	0.4					
4	Left	1.7					
5	Left	0					
6	Left	1.7					
7	Left	1.2					
11	Right/Left	0.5					
12	Right	2.3					

Table 7. Rate of advance (deposit) and retreat (erosion) in volume per year as calculated from the change in area for the surveyed cross sections.

Pins

Bank Type	n	Average Rate of Change (cm/year)	Minimum Rate of Change (cm/year)	Maximum Rate of Change (cm/year)	σ (cm/year)	± σ (cm/year)
1a	19	-23.9	-4.3	-63.0	15.5	(-39.4 to -8.4)
1b	2	-31.1	-30.7	-31.4	0.5	(-31.6 to -30.6)
2	5	2.2	7.7	-2.7	4.4	(-2.2 to 6.6)
3	2	8.5	12.6	4.4	5.8	(2.7 to 14.3)

Cross Sections

Bank Type	n	Average Rate of Change (cm/year)	Minimum Rate of Change (cm/year)	Maximum Rate of Change (cm/year)	σ (cm/year)	± σ (cm/year)
1a	8	-12.2	0.0	-21.2	6.5	(-19.8 to -5.7)
1b	0	nd	nd	nd	nd	nd
2	8	-1.1	9.4	-8.6	6.6	(-7.7 to 5.5)
3	6	10.1	20.0	-13.0	11.7	(-1.7 to 21.8)

Table 8. Compares rate of retreat (-) and advance (+) determined from the pins and cross sections .

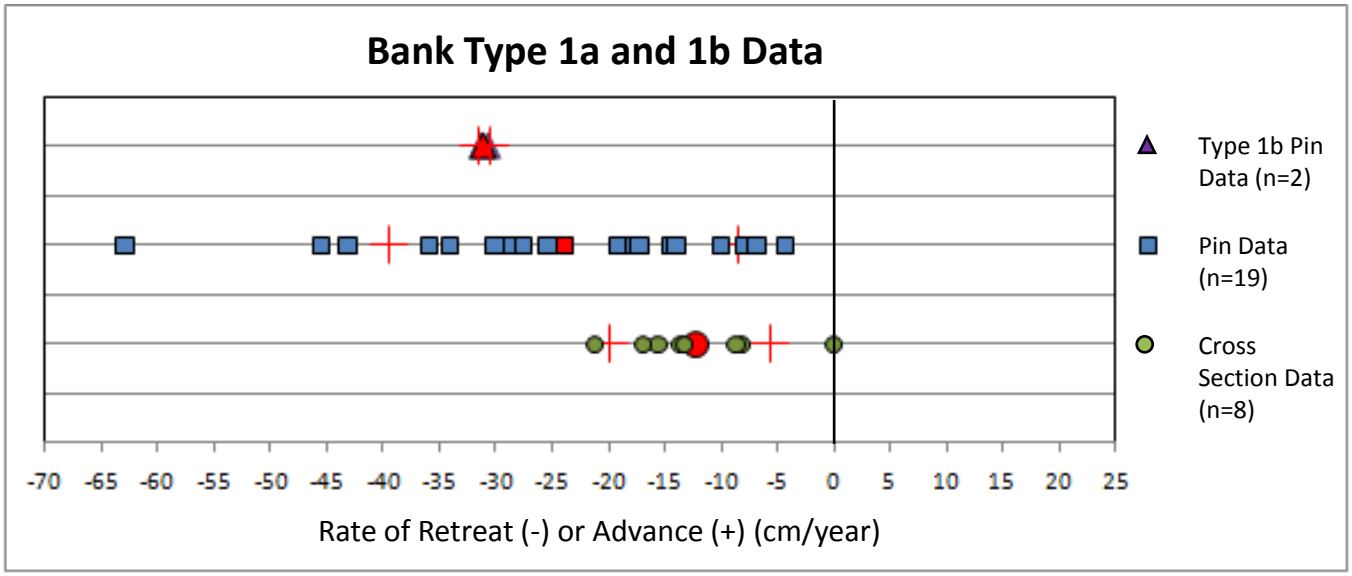

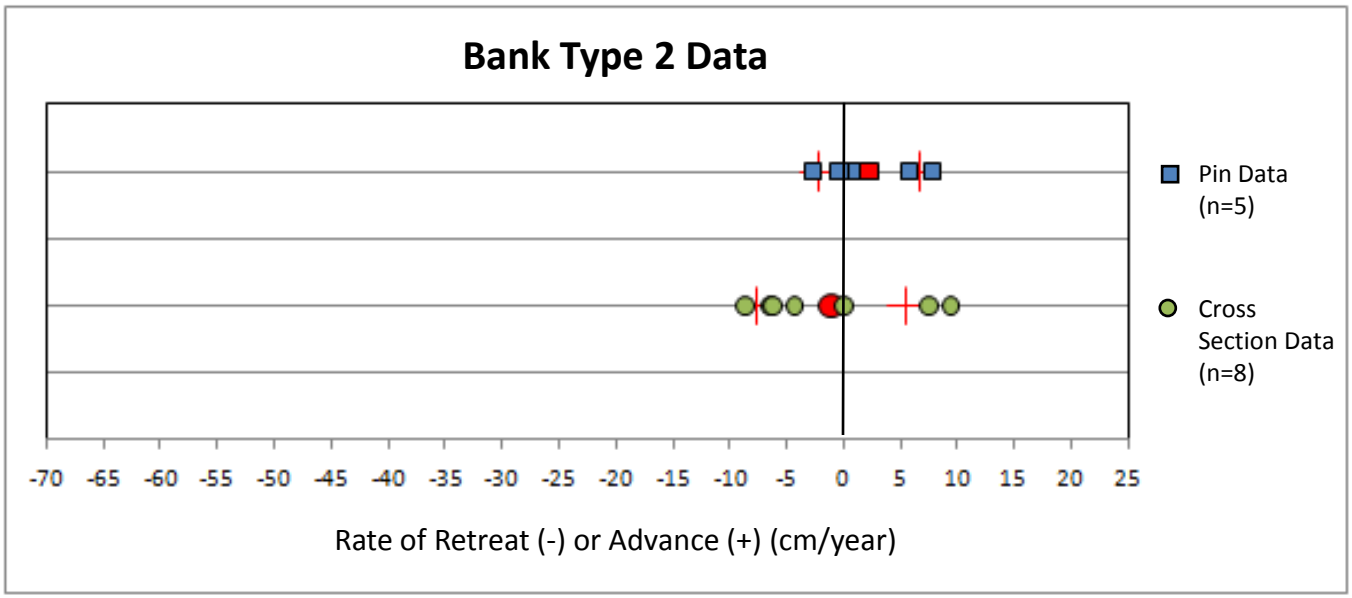

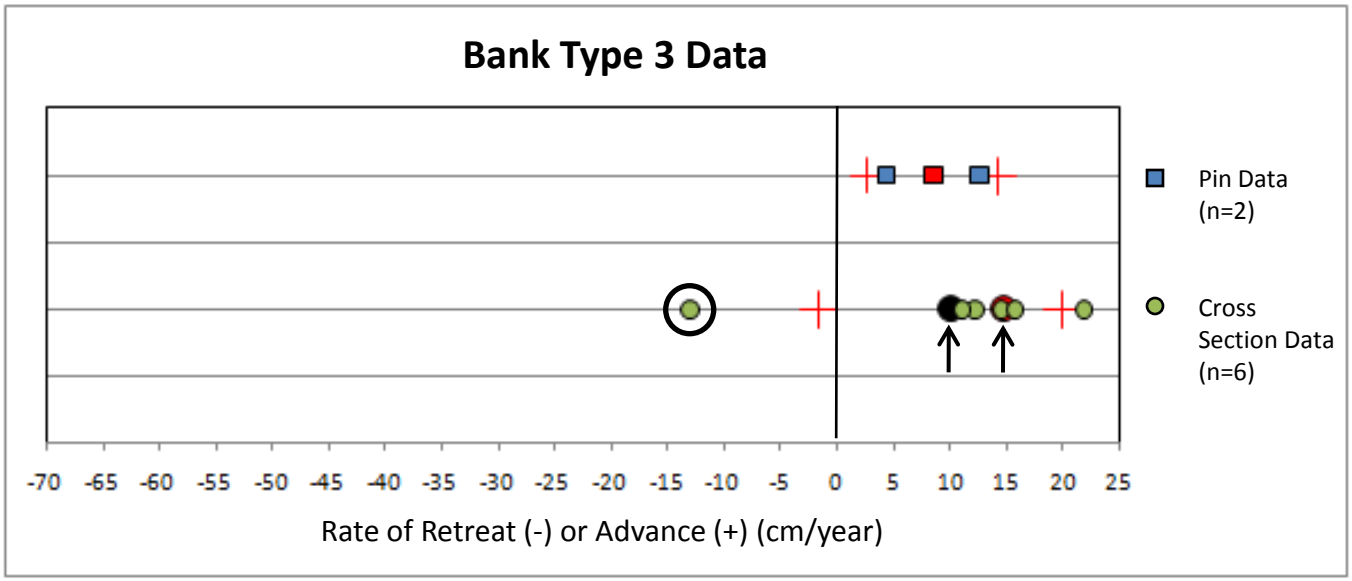

Figure 27. Series of graphs showing both the pin and cross section data for a given bank type. Pin data collected over 1-2 years. Cross section data was collected over 6 years. Red data point represents the average for that series. Red lines show +/- 1 standard deviation for each series. Two averages for Cross Section Data shown with arrows in bottom graph. Arrow to the right shows the average without the circled outlier, arrow to the left shows the average with all values included.

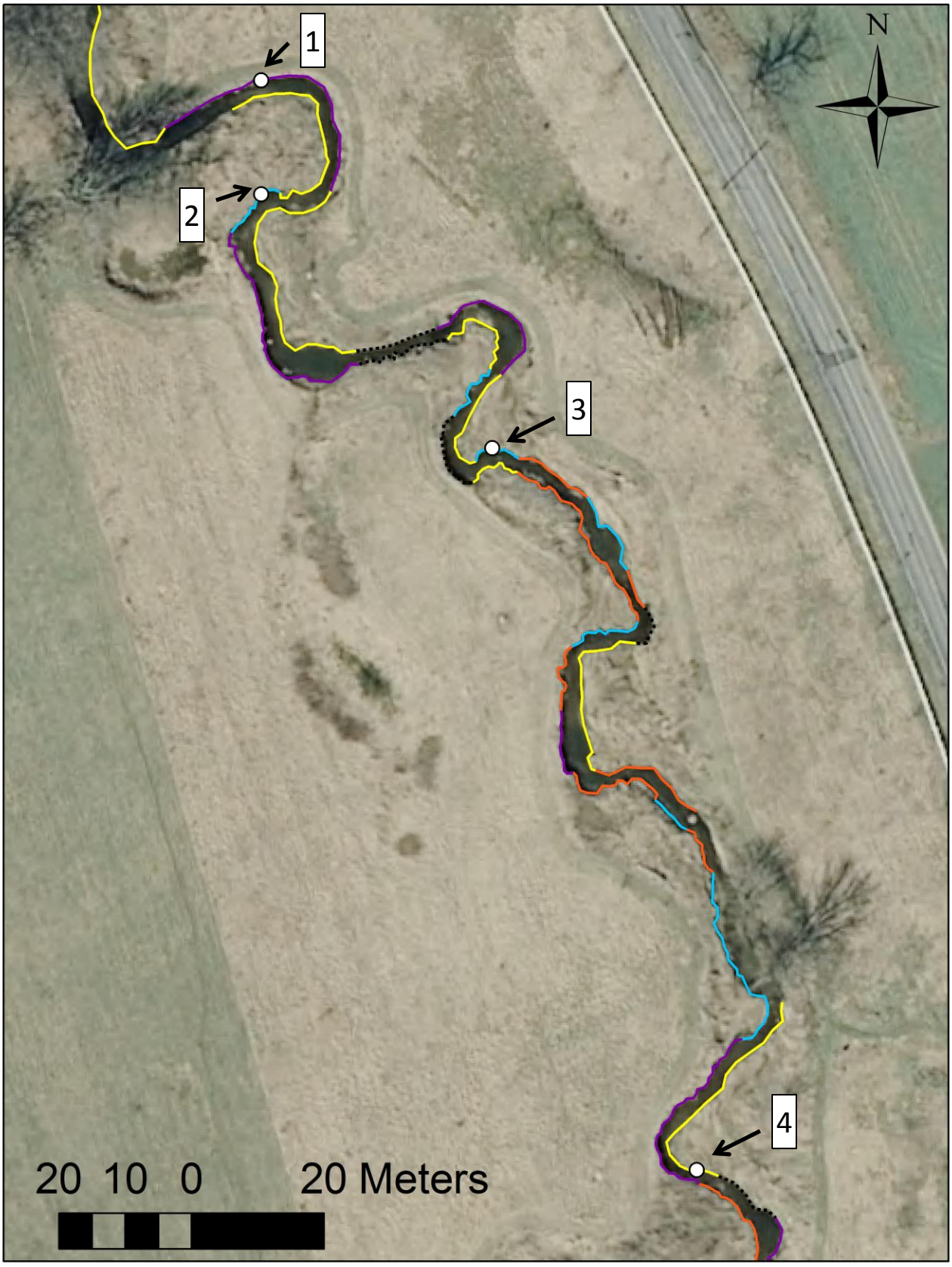

Figure 28. Map showing the sediment sample collection sites. Site 1, in bank Type 1a (purple) was collected and analyzed by Zach Stein in 2007, Sites 2 and 3, both in bank Type 1b (blue), were collected by Dr. Merritts and Dr. Walter and analyzed by Laura Kratz in 2010. Site 4, in bank Type 3 (yellow) was collected by Dr. Merritts and Dr. Walter in 2010 and analyzed by Laura Kratz.

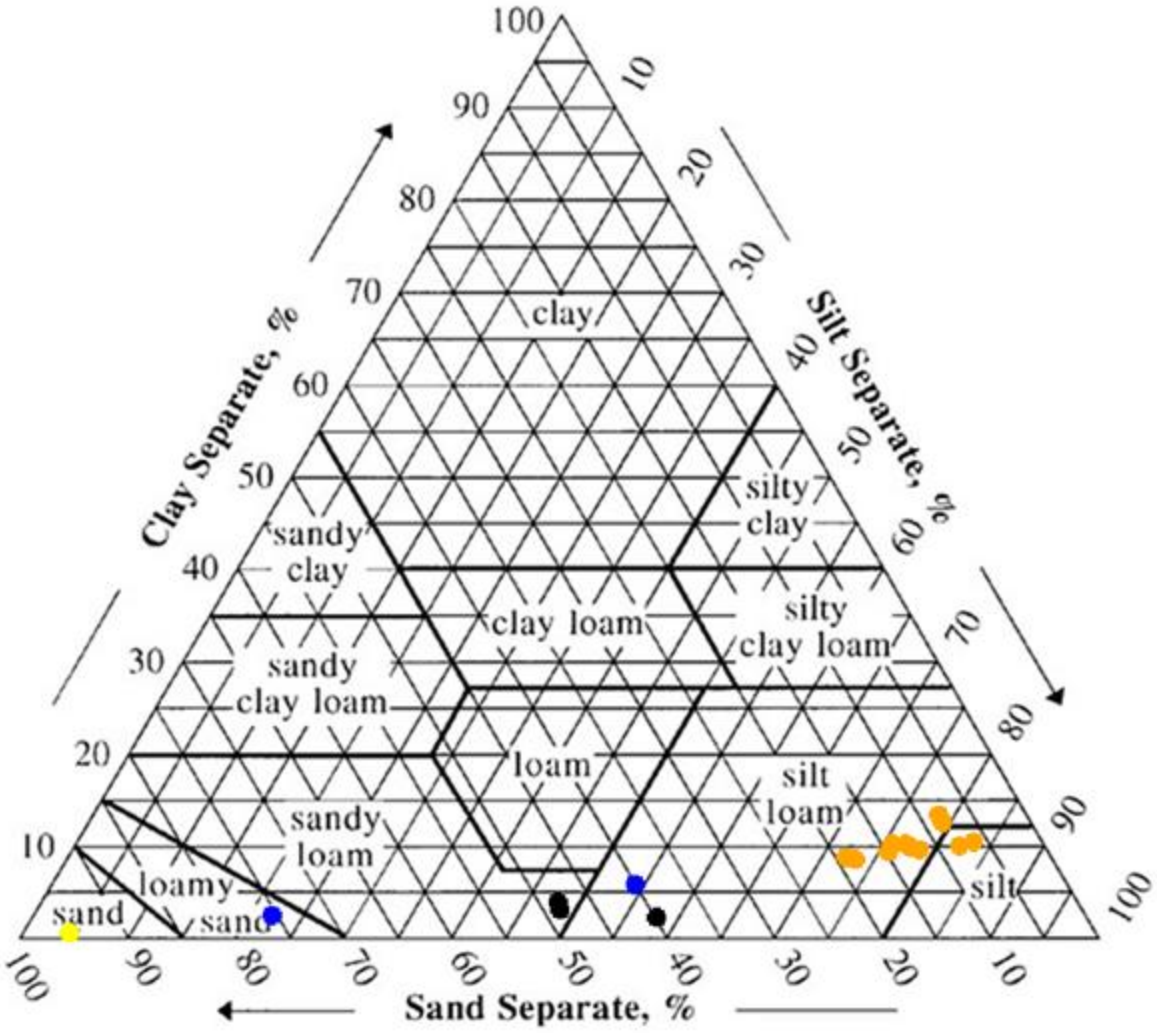

● - Type 1a (Collection site 1)
● - Pre-settlement black layer (Collection site 1)
● - Type 1b (Collection sites 2 and 3)
● - Type 3 (Collection site 4)

Figure 29. Ternary soil texture diagram for percent sand, silt, and clay by mass.

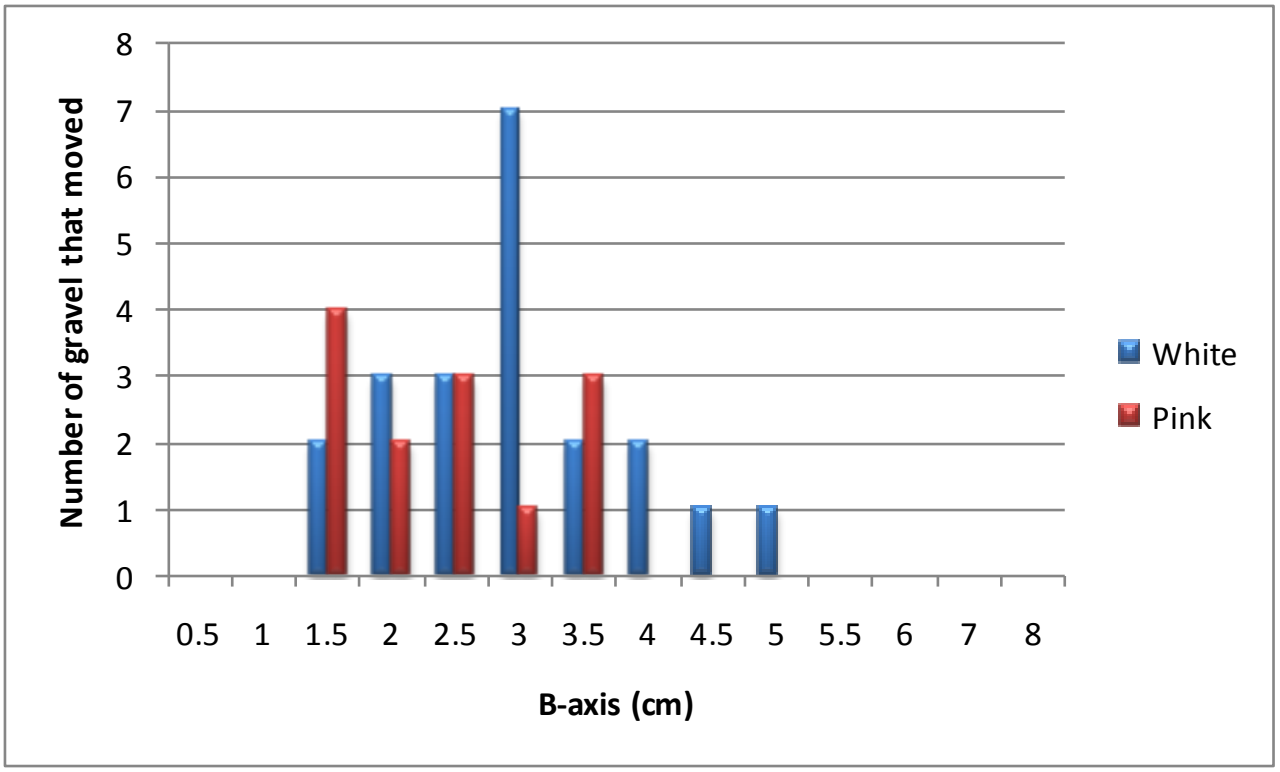

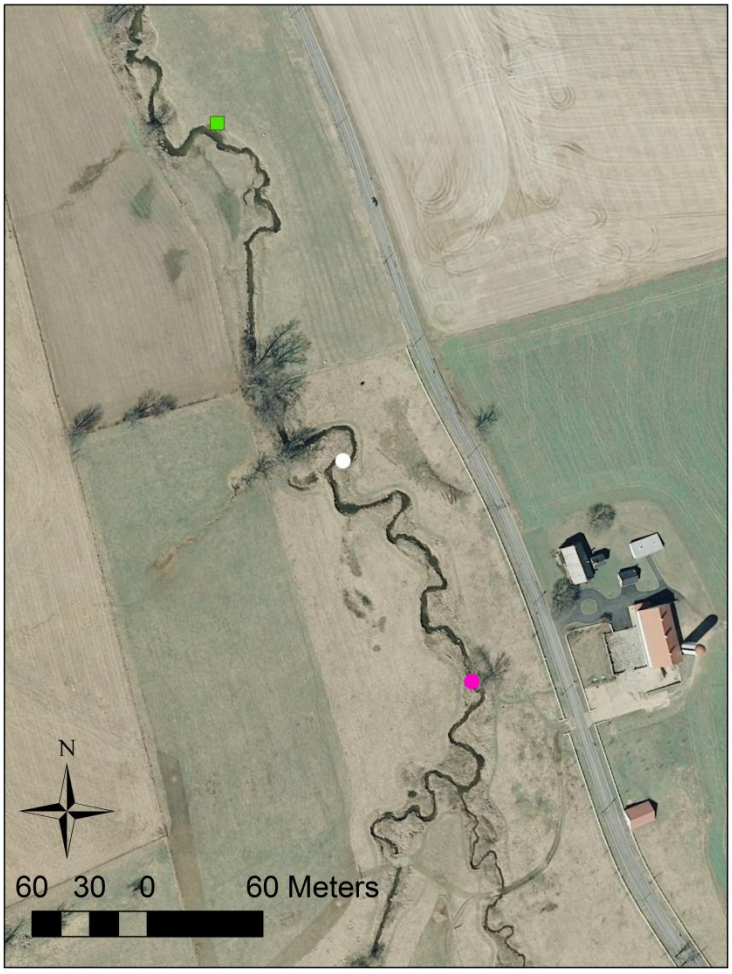

Figure 30. (Above) Size and number of gravel clasts that moved during high flow events between September and December, 2010. (Left) Map showing the location of gravel test sites. Pink dot corresponds with pink gravel, while dot corresponds with white gravel. Green square shows the downstream gauge station on the main stem of BSR.

Erosion

Bank Type	Total Bank Length (m)	Average Bank Height (m)	Area (m^2)	Volume per Year (m^3/year)	Total Volume per Year (m^3/yr)	Tons per year
1a	765	1.2	918.0	219.4	283.8	312.8-406.7
1b	187	1.1	205.7	64.4		

Method 1: Volume and mass of eroded sediment calculated using average bank height, total length, and average erosion rate from pins. Mass is calculated from volume using bulk density (1000 – 1300kg/yr).

Bank Type	Total Bank Length (m)	Average Bank Height (m)	Area (m^2)	Volume per Year (m^3/year)	Total Volume per Year (m^3/yr)	Tons per year
1a	765	variable	992.3	237.2	300.1	330.8-430.1
1b	187	variable	201.2	63.0		

Method 2: Volume and mass of eroded sediment calculated using length and height of each mapped stream segment and average erosion rate from pins. Mass is calculated from volume using bulk density (1000 – 1300kg/yr).

Bank Type	Total Bank Length (m)	Total Area (m^2 per 6 years)	Average Area per year (m^2/yr)	Volume per Year (m^3/year)	Tons per year
1a	952	8.6	0.7	158.7	174.9-227.4
1b					

Method 3: Volume and mass of eroded sediment calculated using the cross-sections to measure an average area of erosion for the cross sections, then multiplying by the total length of Type 1 and 1b.

Deposition

Method 3: Volume and mass of deposited sediment calculated using the cross-sections to measure an average area of erosions for the cross sections them multiplying by the total length of Type 3.

Type	Total Bank Length (m)	Total Area (m^2 per 6 years)	Average Area per year (m^2/ yr)	Volume per year (m^3/year)	Tons per year
3	671	6.5	0.15	100.7	111.0-144.3

Tables 9 – 12. Tables explaining the three different methods of calculating tons of eroded sediment per year and one table for deposition. Each table shows the data needed for the calculations.

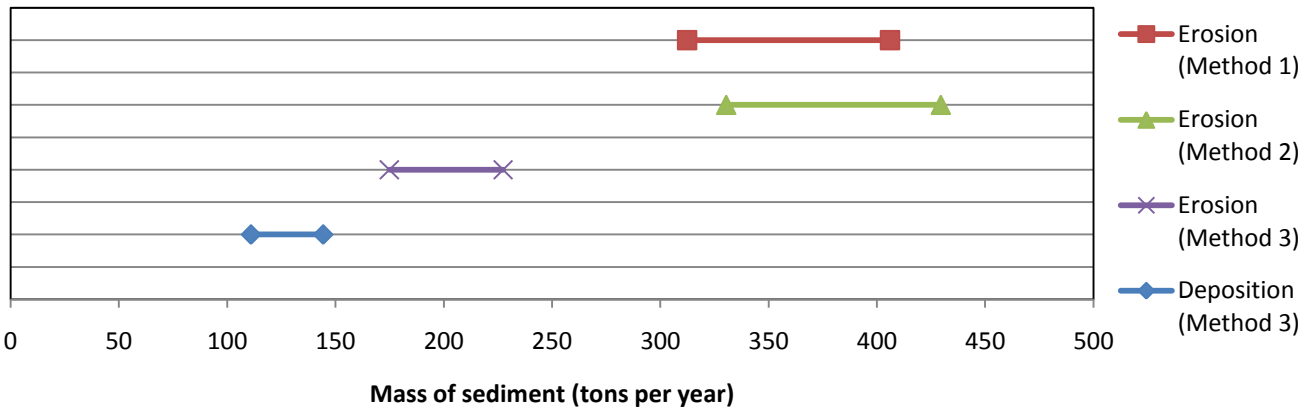

Figure 31. Graph comparing the average amounts of sediment eroded and deposited per year calculated through different methods.

APPENDIX 1

Prepared by Michael Rahnis

Cross-Section Survey Methodology

2004 Survey

A stream cross-section survey at the Big Spring Run restoration site was initially conducted by LandStudies, during Fall of 2004, using a Total Geodetic Station. Survey control consisted of five iron rods with yellow caps placed flush with the ground. Additionally, a surveyor's mag-nail shown on restoration designs was located in pavement next to a storm grate. The elevation for the nail is given as 326.61 feet (NAVD88). The nail is not believed to have been observed during the cross-section survey.

Data were provided by LandStudies in a text file containing local grid coordinates and codes for both the cross-sections and the benchmarks. A total of twelve cross sections were surveyed. In Fall 2009 LandStudies assisted us by staking out the cross section end-points and placed rebars at those locations.

2010 Survey

F&M resurveyed the cross-sections during April 2010 using a RTK-GPS.

The RTK base was configured to log static data during survey sessions. Northing and Easting was recorded in Pennsylvania state plane, US-feet. Elevation was recorded in NAVD88, US-feet. The static data was differentially corrected using the OPUS service offered by the National Geodetic Survey at NOAA. All data were adjusted to account for the differential correction of the base location.

The RTK rover was used to observe the control points and the ground surface on the lines of cross-section. All five benchmarks and the nail were located and observed for 180 1-second epochs with an RTK-fixed solution. Topographic points were observed for four 1-second epochs with an RTK-fixed solution.

Data Adjustments

Survey data were exported from the job file for import into Excel and ArcGIS. LandStudies original 2004 data was adjusted from its local grid coordinates to Pennsylvania state plane using the similarity method with the five benchmarks in ArcGIS "Spatial Adjustment" tools. The similarity transform scales, rotates and translates the data; it does not change the aspect ratio or skew the data. The adjustment yields a horizontal RMS of 0.02 feet.

Repeated observation of the mag-nail produced results that were consistently within 0.02 vertical feet of the value noted on the plan sheet. Repeated observation of the benchmarks used in the original cross-section survey produced elevations that were consistently higher than those from the original survey, with the exception of one benchmark from which the yellow cap had broken off.

The mag-nail is believed to represent the best available local elevation datum as it is in pavement, whereas the iron rods are driven into soil in a pasture. Therefore a vertical offset of 0.088 feet was added to the 2004 cross-section survey to bring it into close agreement with current survey control, which includes the mag-nail. The vertical offset is the average vertical difference between benchmark elevations observed in 2004 and 2010 for four of five benchmarks, excluding the benchmark with the missing yellow cap.

Cross-section Development

The ArcGIS "Linear Referencing" tools were used to develop the cross-sections. In ArcGIS line features were created to connect the cross-section end-points. These were converted to route layers against which features can be addressed. The cross-section observations were addressed, or in this case orthographically projected, onto the lines of section using orthographic projection and output to a new table. The table was exported to a comma-separated value file and imported into Excel for plotting.

Bank Type	Minimum Height (m)	Maximum Height (m)	σ	Average Height (m)
1a	0.6	1.7	0.29	1.2
1b	0.8	1.3	0.18	1.1
2	0.2	2.7	0.43	1
3	na	na	na	na

Appendix 2. Additional information about the bank height for the different bank types

Appendix 3. Cross Sections

Cross Section 1

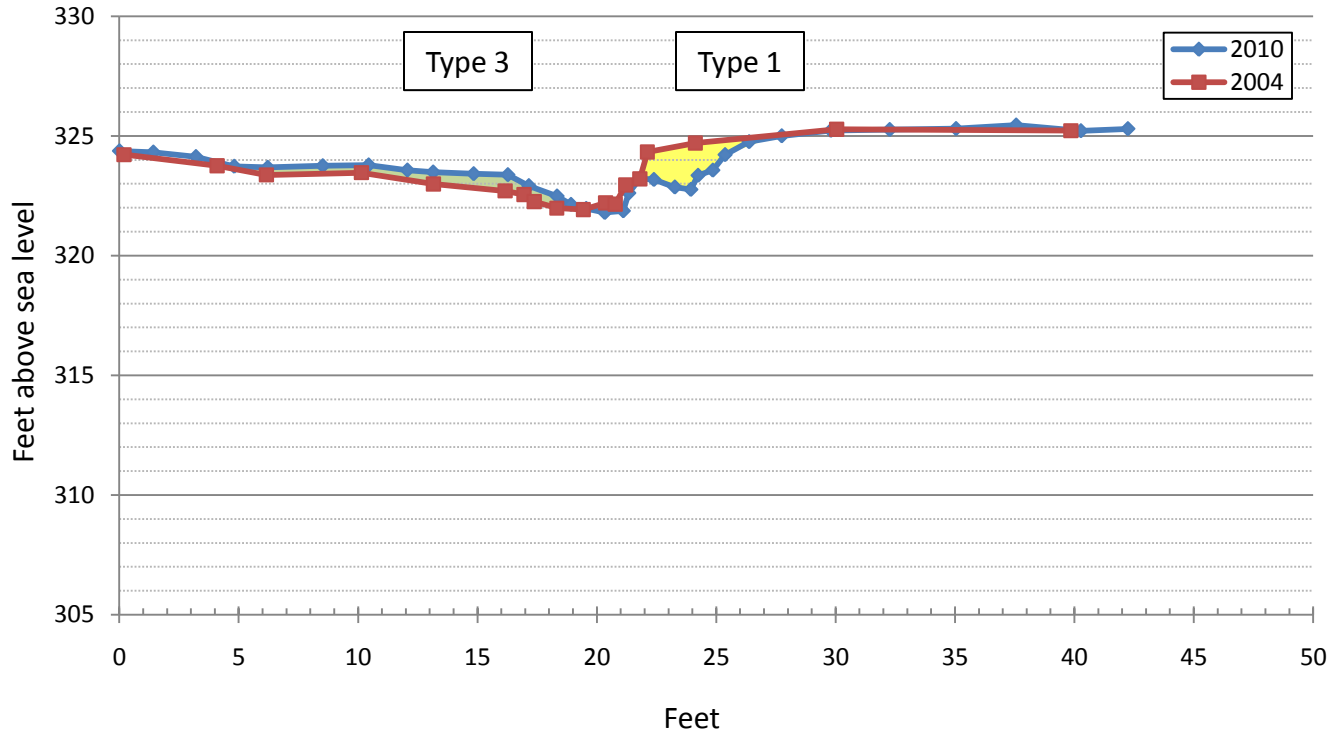

Cross Section 2

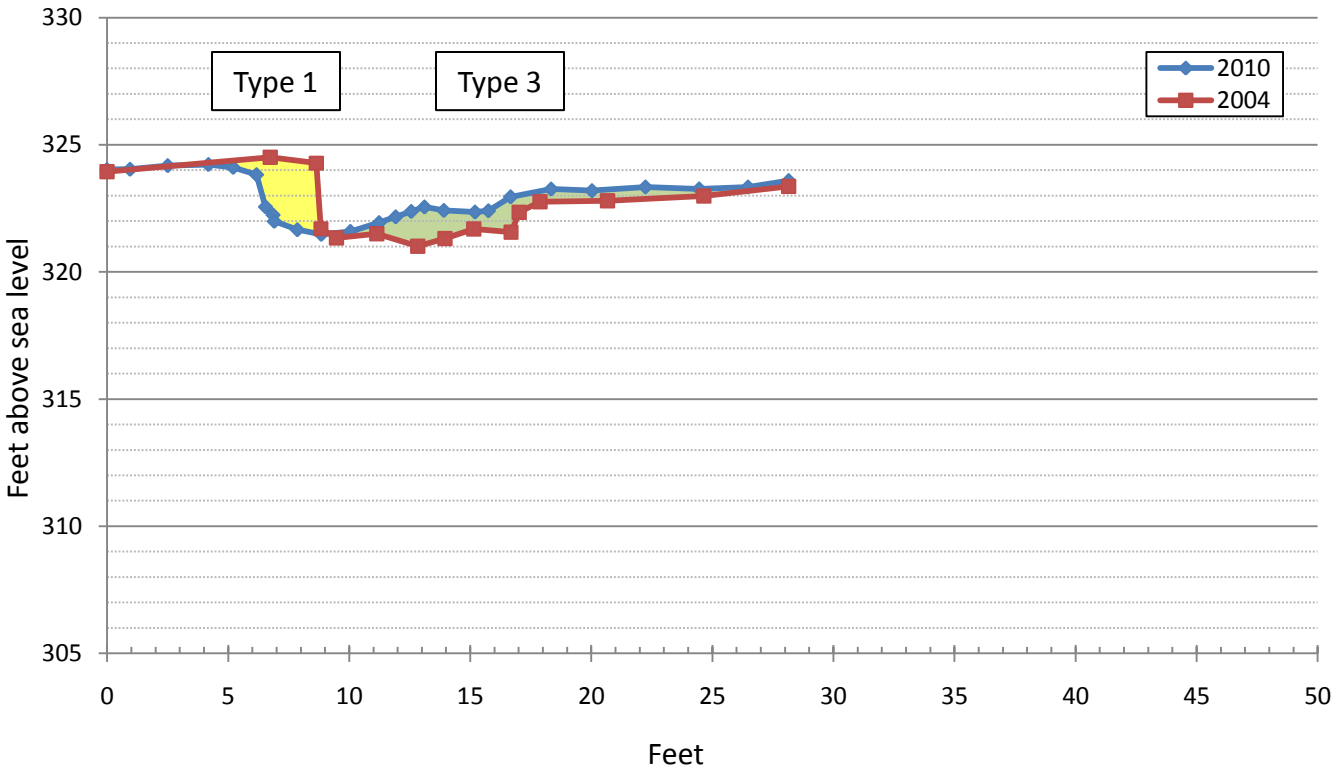

Appendix _. Cross Sections (Continued)

Cross Section 3

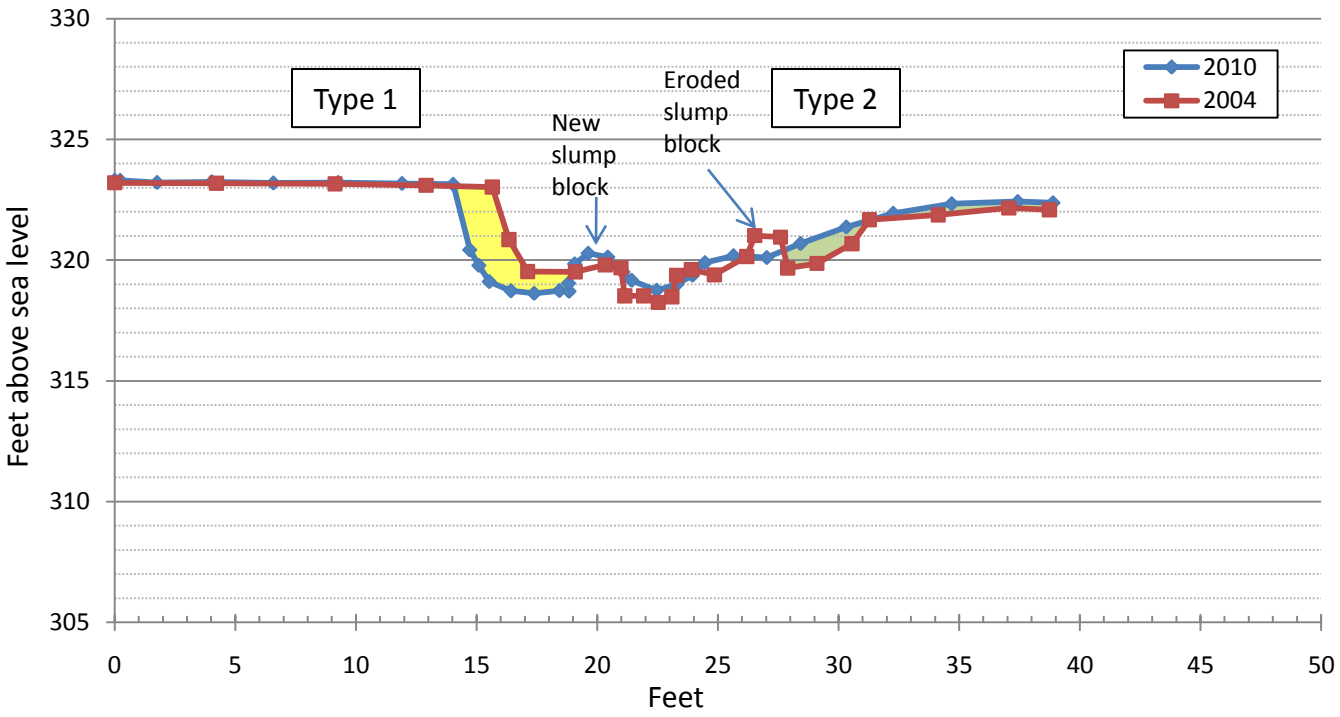

Cross Section 4

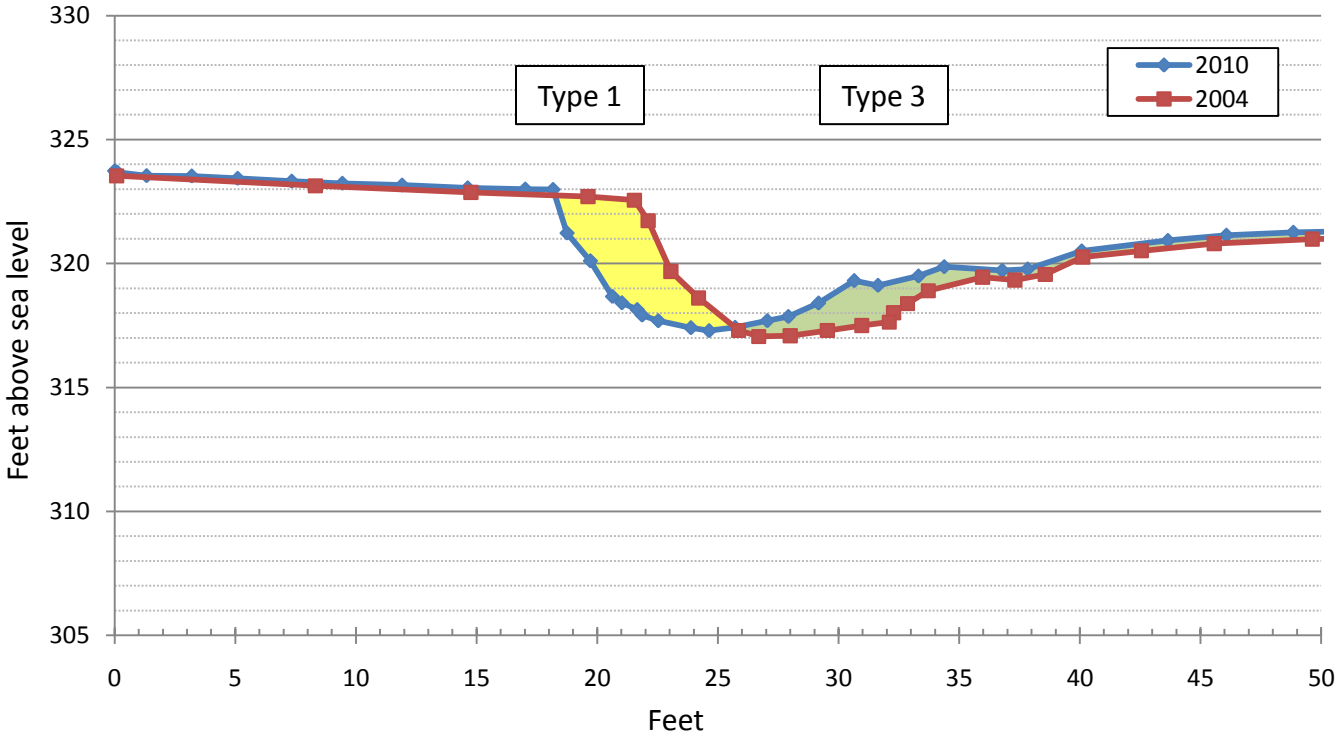

Appendix 3. Cross Sections (Continued)

Cross Section 5

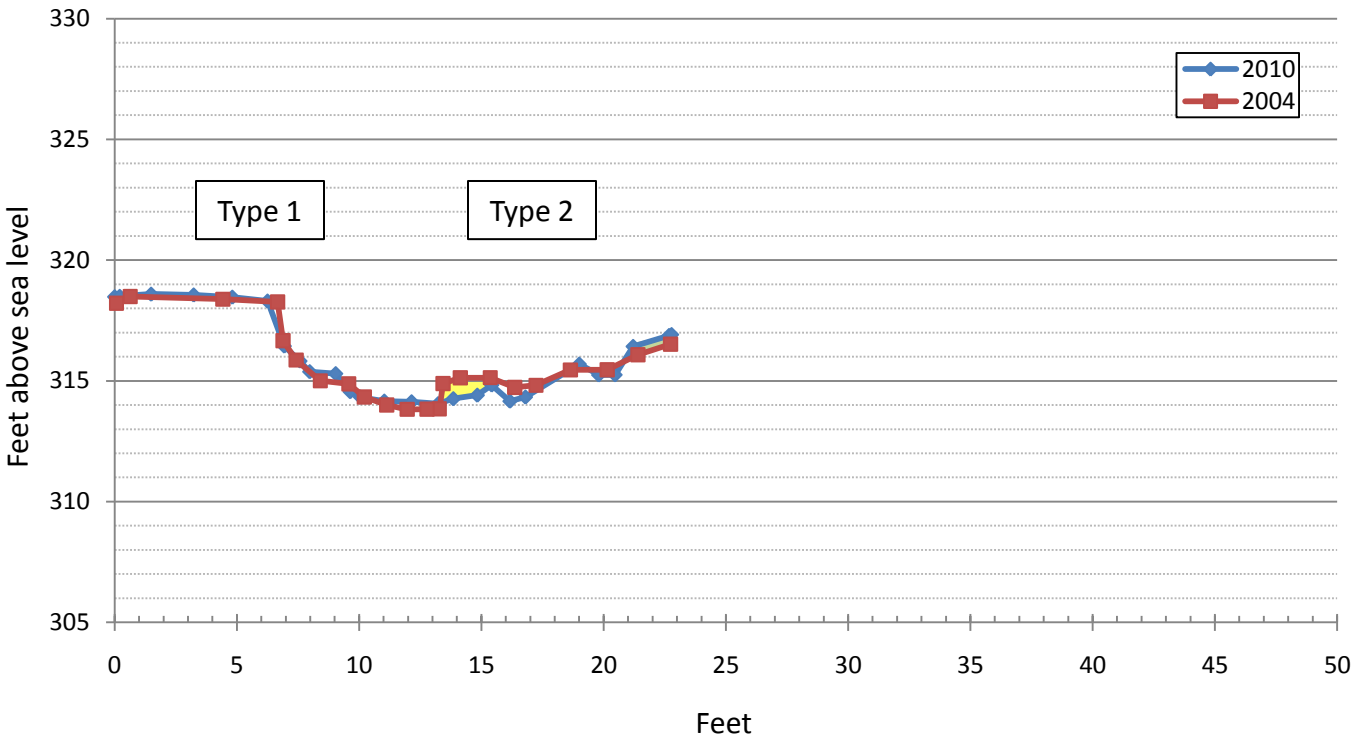

Cross Section 6

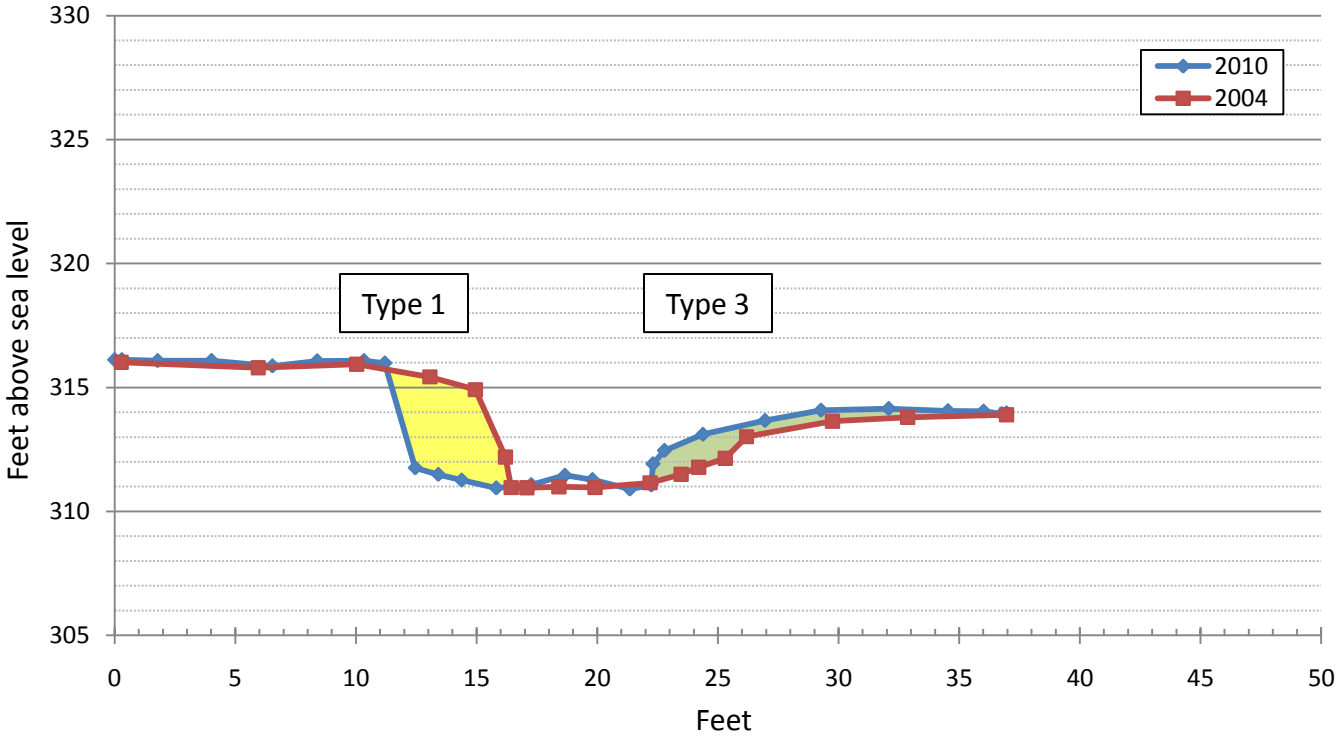

Appendix 3. Cross Sections (Continued)

Cross Section 7

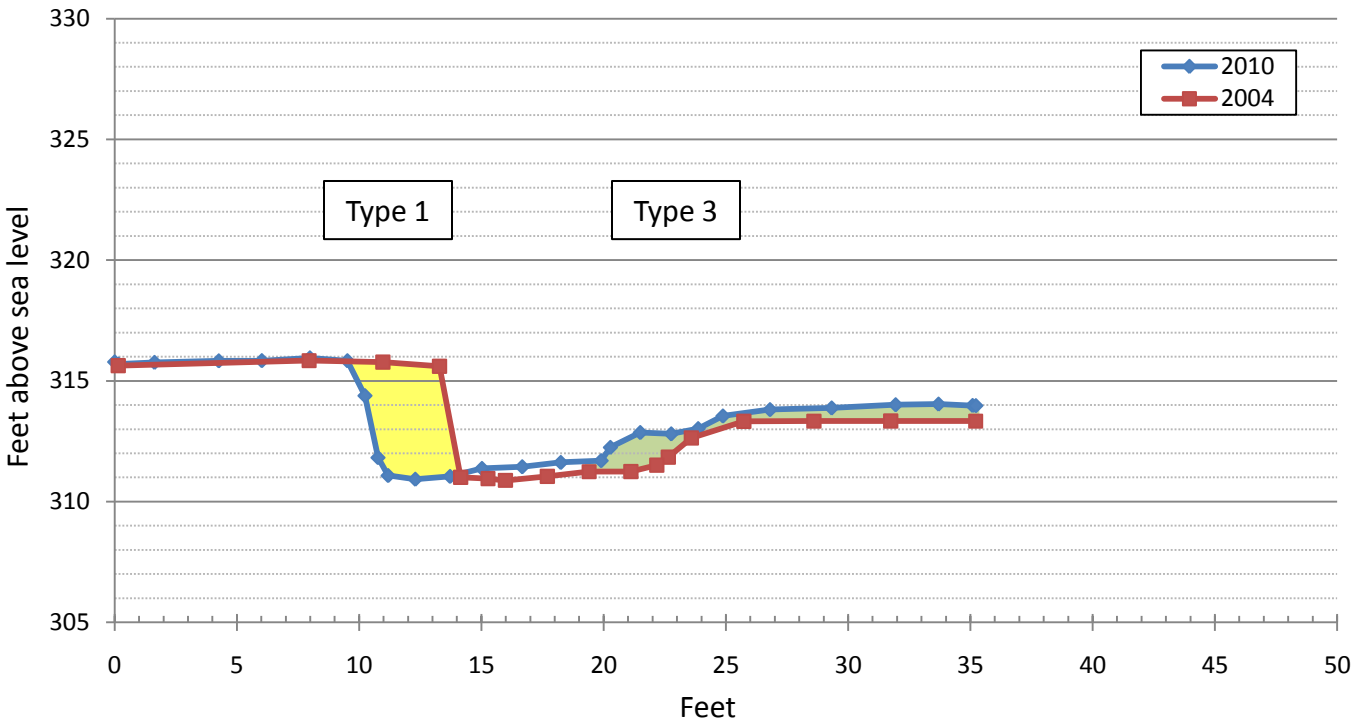

Cross Section 8

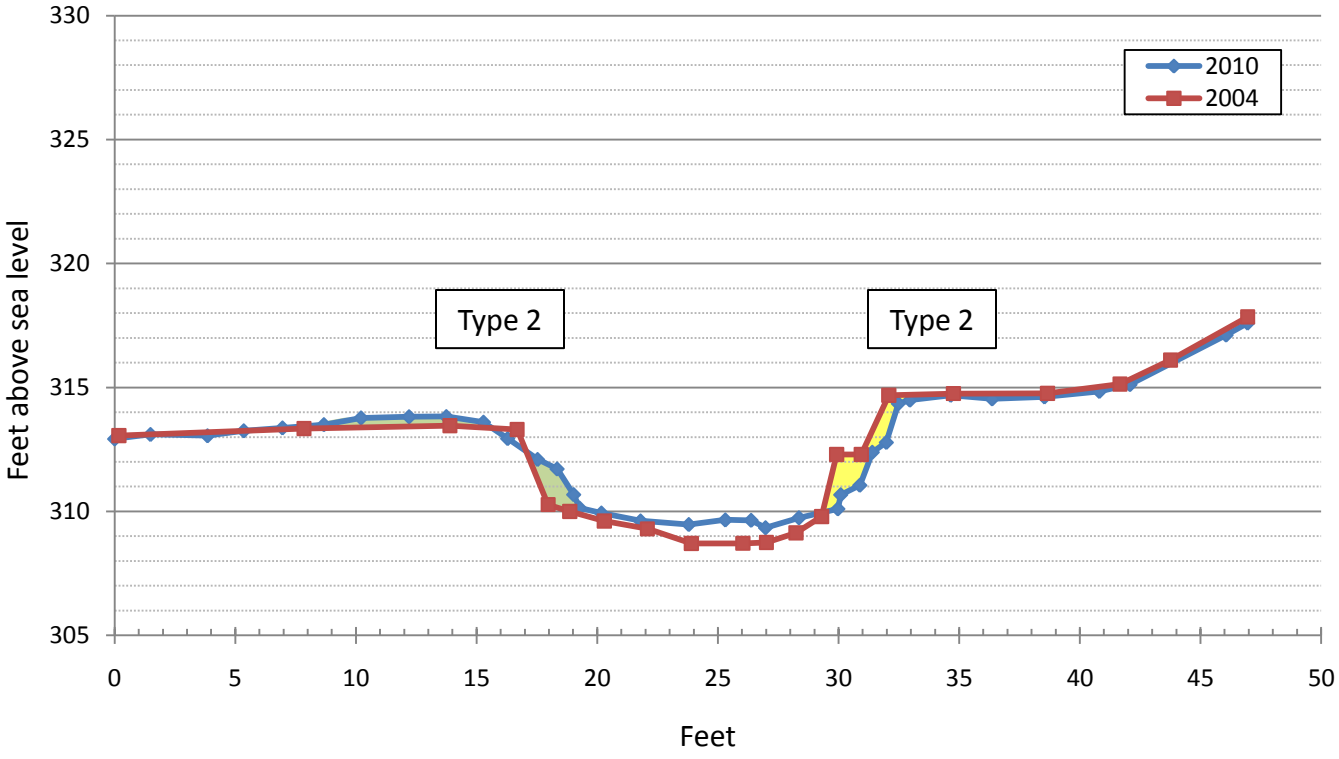

Appendix 3. Cross Sections (Continued)

Cross Section 9

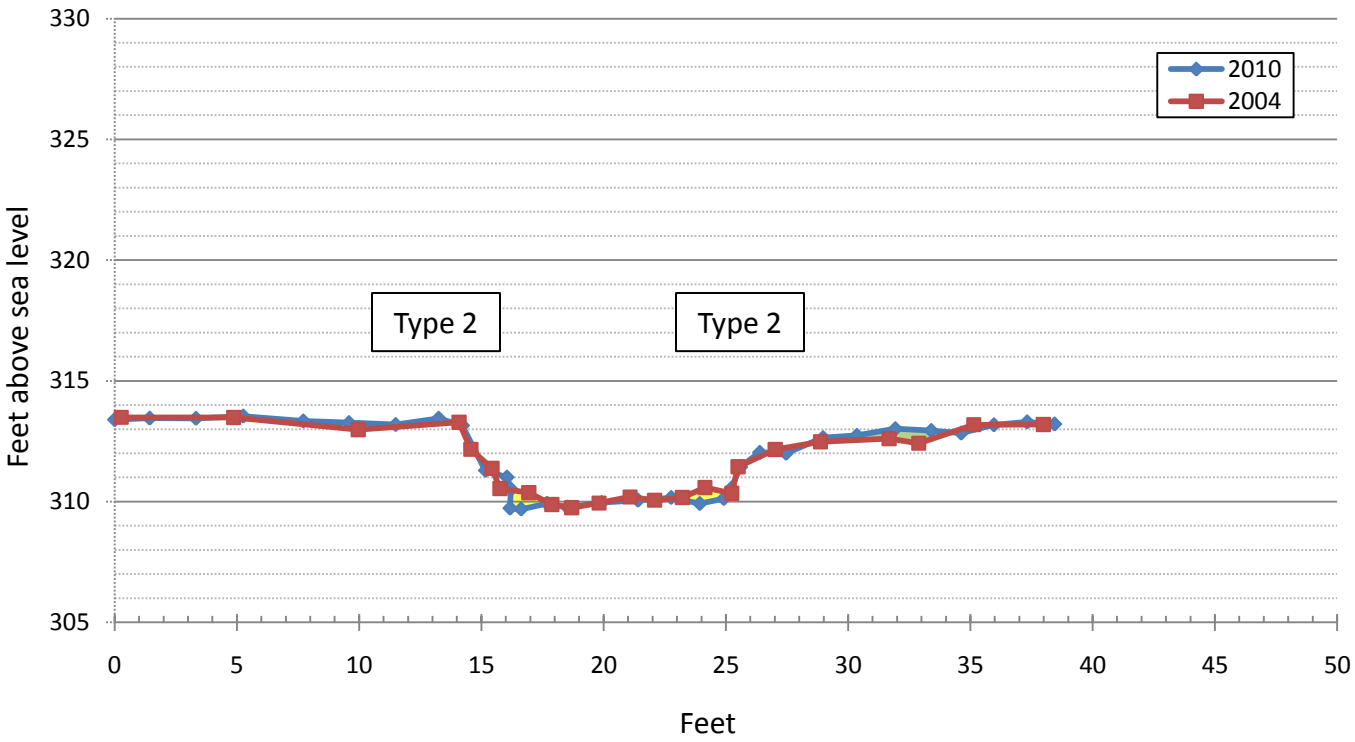

Cross Section 10

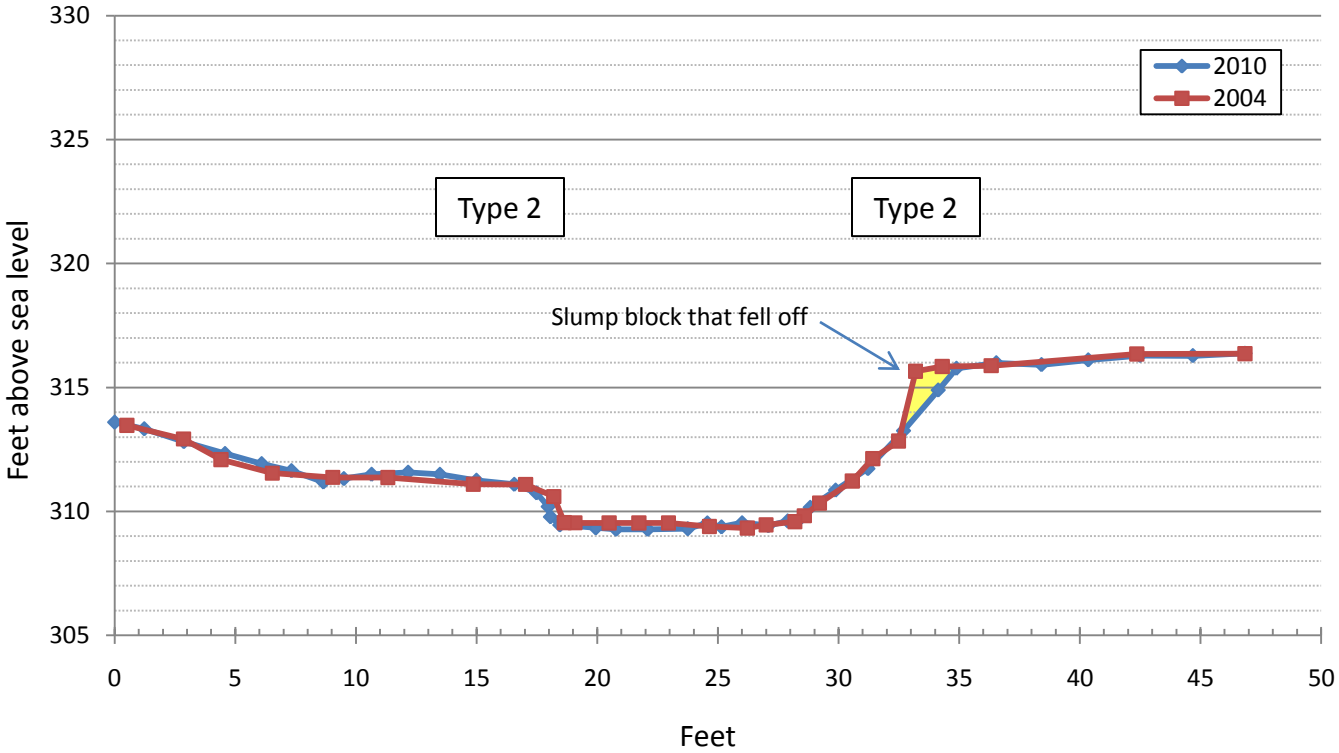

Appendix 3. Cross Sections (Continued)

Cross Section 11

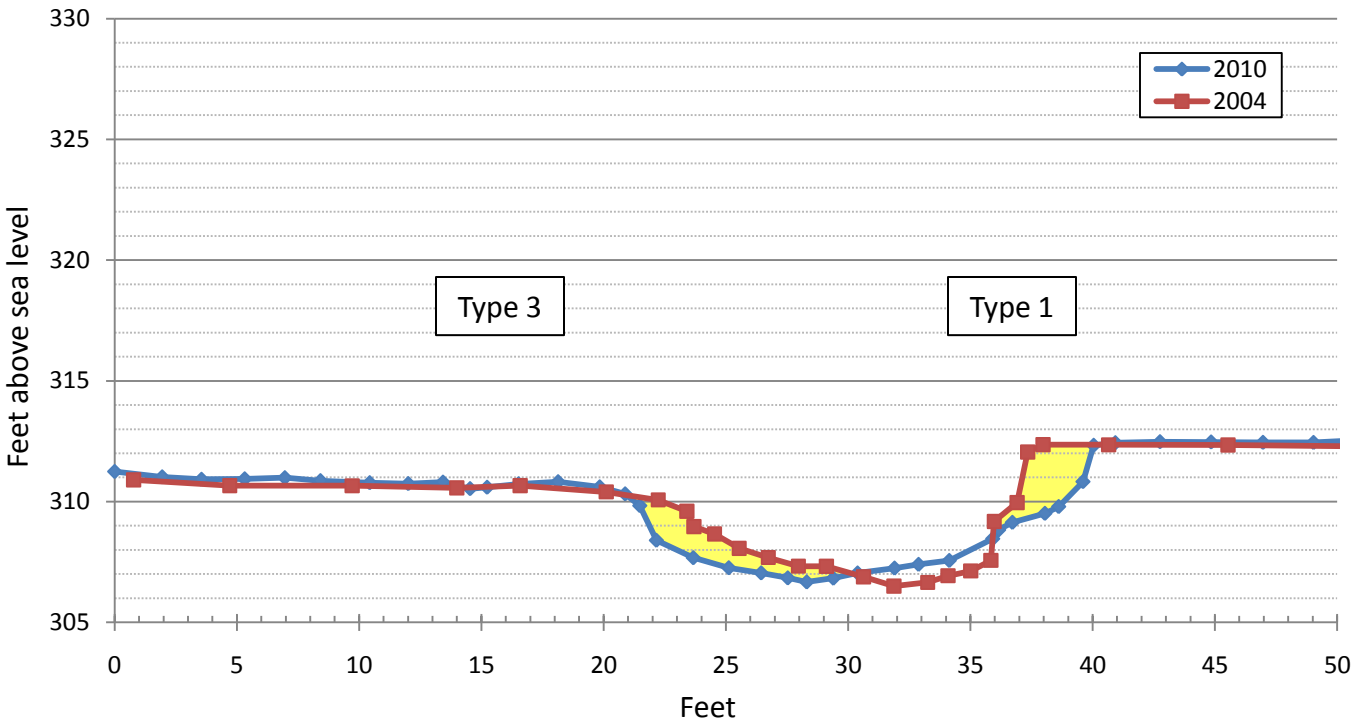

Cross Section 12

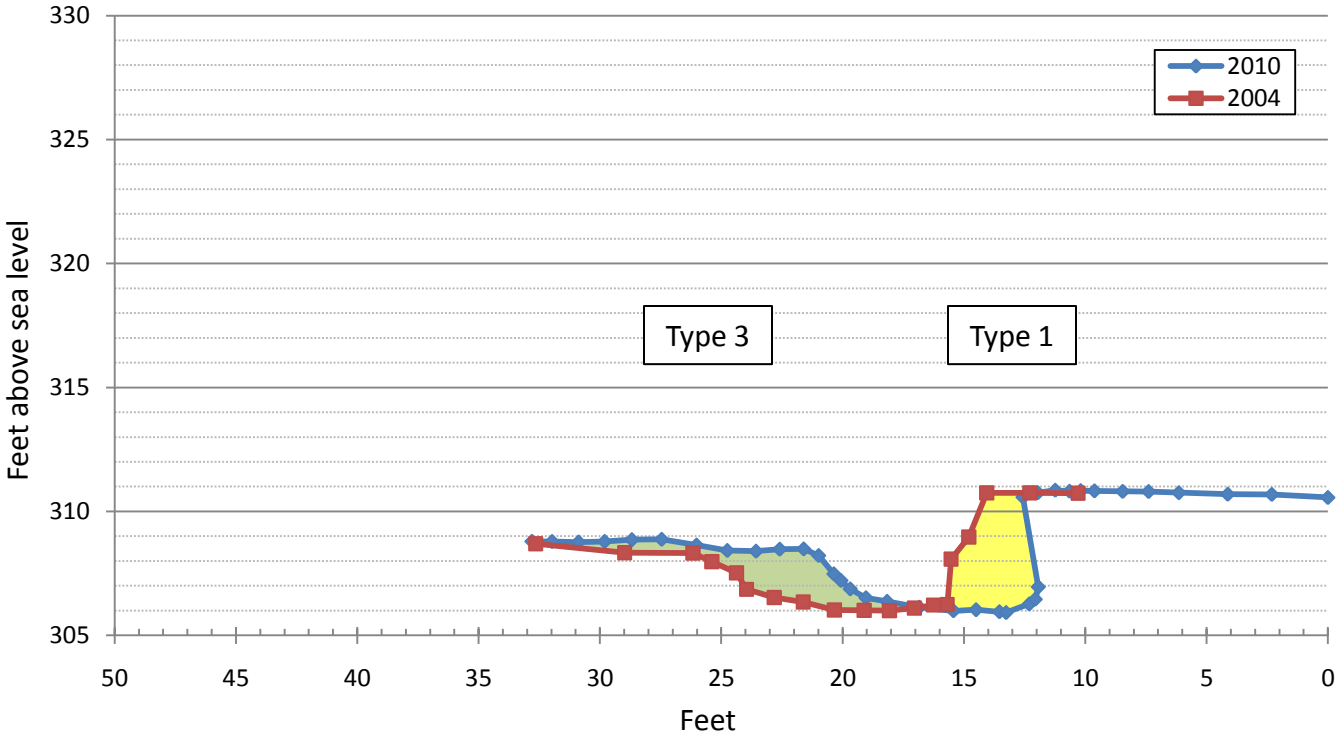

Appendix 4. Table showing methodological uncertainty

Methodology	Dimension	Half-range (ft)	Source	Typical value (ft or ft^2)	Typical change value (ft^3)	Typical measurement period (yr)	Range (+/- ft^3)	Uncertainty (1-sigma %, assumed triangular distribution)	Uncertainty (1-sigma %, assumed normal distribution)
Pins	Horizontal	0.07	Pin measurement	1	6	1 yr	2.6	0.18	14.6
	Vertical	0.13	Bank height measurement	6					
	Vertical, longitudinal	0.13	Extrapolation to unit stream length on irregular surface	1					
Cross Section	Horizontal	0.03	Kinematic survey horizontal RMSE	50	30	1-2 yr	23.2	0.32	25.8
	Vertical	0.07	Kinematic survey vertical RMSE	6					
	Vertical, longitudinal	0.13	Extrapolation to unit stream length on irregular surface	1					